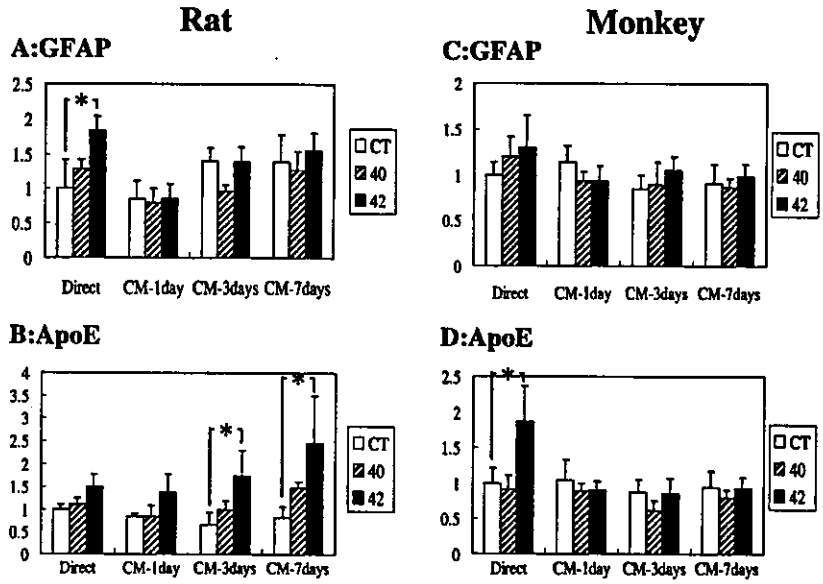

Fig. 4. Immunoreactive bands shown in Fig. 3 were quantified, and the resulting density data were compared to those measured from blots containing extracts from control cultures (* $P < 0.02$). In rat astrocyte cultures ($N = 6$) (A, B), direct treatment with Aβ42 significantly increased GFAP expression levels (A). Direct treatment with Aβ42 increased ApoE expression levels, and furthermore, treatment with conditioned media from cortical cultures treated with Aβ42 for either 3 or 7 days significantly increased ApoE expression (B). The degree of ApoE increase was directly correlated with the number of days the cortical cultures were treated with Aβ. In monkey astrocyte cultures ($N = 6$) (C, D), direct treatment with Aβ42 slightly increased GFAP expression (C). Direct treatment with Aβ42 significantly increased ApoE expression (D). Labeling conventions as in Fig. 3.

of the conditioned-media treatments (i.e., Aβ40, Aβ42, or duration of Aβ exposure), failed to affect ApoE expression levels in monkey astrocyte cultures (Fig. 4D).

4. Discussion

Aβ was previously shown to induce neuronal apoptosis, activate GSK3β, and lead to the accumulation of newly synthesized intracellular Aβ in APP-transfected cells (Cardoso et al., 2002; Ivins et al., 1999; Loo et al., 1993; Mattson et al., 1998; Morishima et al., 2001; Troy et al., 2000; Takashima et al., 1998; Yang et al., 1999). Although these studies shed much light on the various phenomena induced by Aβ, the initial effects of or disturbances caused by Aβ accumulation in the brain remain unknown; astroglial responses primarily occur, or neuronal injuries primarily happen. In the brain, small quantities of Aβ typically accumulate with age; and in some cases, this accumulated Aβ aggregates, causing Aβ-associated pathologies such as AD (Selkoe, 1991). In the present study, we sought to clarify events that may occur early on during the initial stages of Aβ accumulation and aggregation. This was achieved by assessing cultured neuronal cells for signs of apoptosis and altered expression of certain proteins following long-term treatment (14 days) with relatively low concentrations of "no pre-aggregating" forms of Aβ.

In both rat and monkey cortical cultures, Aβ did not significantly decrease or increase expression of caspase-3 or the neuron-related proteins synaptophysin, APP-βCTF, and GSK3β (Figs. 1, 2A–C,F–H, data not shown for caspase-3). These results indicate that Aβ had no effect on neurons during the initial stages of Aβ accumulation and aggregation, indicating that Aβ and its subsequent accumulation and aggregation did not appear to disrupt the formation of synapses.

On the other hand, Aβ treatment increased the expression of the astrocyte-related proteins GFAP and ApoE in both rat and monkey cortical cultures (Fig. 1D,E,I,J), indicating that astroglia, rather than neurons, may be the first neural cells affected by the initial accumulation and aggregation of Aβ in the brain. During the initial stages of Aβ accumulation, therefore, one would intuitively expect to detect astroglial responses (e.g., changes in the expression of astroglia-related proteins) before neuronal responses (e.g., neuronal injury or apoptosis).

The astroglial responses to Aβ differed somewhat in rat and monkey cortical cultures, suggesting possible species differences in how astrocytes react to the accumulation and aggregation of Aβ. In rat cortical cultures, Aβ treatment tended to increase GFAP and ApoE expression levels to a greater degree than in monkey cortical cultures (Figs. 1 and 2D,E,I,J). This finding suggests that rat neuronal cells may be more sensitive to Aβ (thus requiring a greater astroglial response), whereas monkey neuronal cells may be more resistant to Aβ (thus requiring a lesser astroglial response). Cynomolgus monkeys are old world monkeys classified as nonhuman primates and are more similar to humans than rats. Extrapolation of these results, therefore, to humans leads to the prediction that neurons in the human brain may be more resilient than previously thought and may resist

damage during the early stages of Aβ accumulation, thereby allowing astrocytes more time to react and remove excess Aβ from the brain before neuronal injury can occur.

The astroglial responses to different forms of Aβ also differed. In both rat and monkey cortical cultures, Aβ42 treatment increased GFAP and ApoE levels to a greater extent than in cultures receiving Aβ40 treatment (Figs. 1 and 2). Several studies have shown that Aβ42 is more closely associated with AD pathogenesis than Aβ40 (Burdick et al., 1992; Jarrett et al., 1993; Suzuki et al., 1994; Younkin, 1994). These studies are consistent with our results that Aβ42 induced a much stronger astroglial response than did Aβ40 (Figs. 1 and 2).

We also investigated whether neuron-derived soluble factor(s) may influence astrocytic responses to Aβ. This was addressed by treating astrocyte cultures with conditioned media from neuronal cultures previously treated with Aβ (see Section 2 for details). In rat astrocyte cultures, direct Aβ treatment increased GFAP expression significantly, and ApoE expression also increased with direct Aβ treatment (Figs. 3A and 4); ApoE expression, however, not significant. Furthermore, ApoE expression increased significantly in response to treatment with conditioned medium from cortical cultures exposed to Aβ for either 3 or 7 days (Figs. 3A and 4B). These results indicate that rat astrocytes themselves can be directly activated by Aβ and then increase ApoE expression, but expression of ApoE may be also influenced by an as of yet unidentified soluble factor(s) from neurons treated with Aβ. In monkey astrocyte cultures, only direct Aβ treatment increased both GFAP and ApoE expression, although the increase in GFAP was not significant (Figs. 3B and 4C,D). Similar to the case with rat astrocytes, monkey astrocytes can also be directly activated by Aβ. Unlike with rat astrocytes, ApoE expression in monkey astrocytes is only induced directly by Aβ. Thus, in the monkey brain, astrocytes may remove Aβ without requiring induction by neuronal signals, suggesting that possible species differences exist in the astrocytic responses to Aβ and in the mechanisms underlying these responses. From the study of cortical cultures, it was suggested that rat neuronal cells would be more sensitive to Aβ so that they may require a greater astroglial responses (Figs. 1 and 2D,E,I,J). ApoE is known to play a key role in lipid transport and metabolism, and is also important for neuronal repair (Poirier, 1994). Then rat astrocytes would be stimulated not only directly with Aβ but also by some soluble factors produced by neurons for much ApoE expression. On the other hand, it was also suggested that monkey neuronal cells would be more resistant to Aβ (Figs. 1 and 2D,E,I,J). Then monkey astrocytes would not need to express much ApoE such as rat. This may similarly occur in the human brain in which astrocytes may also be directly activated by Aβ. From these results, we concluded that astrocytes would be activated by Aβ in the early stages of Aβ accumulation and aggregation in the brain, during which time they remove excess Aβ before neurons can be damaged. Our conclusion is consistent with the findings that astrocytes are activated by Aβ, then take up Aβ for degradation (Funato et al., 1998; Matsunaga et al., 2003; Wyss-Coray et al., 2003), and that Aβ also induces astrocytes to produce ApoE and chemokines (Deb et al., 2003; LaDu et al., 2001; Smits et al., 2002). Taken together, these findings show that astroglia are in a pivotal position to reduce Aβ pathogenesis at an early stage, and thus may be a therapeutic target of great interest. Hence, additional studies will be required to clarify astroglial responses to Aβ.

In the present study, we also found species differences in the way astroglia respond to Aβ. Rat astrocytes were more sensitive to Aβ, and as such, may be a useful model to further investigate astroglial responses induced by Aβ. However, since the mechanism underlying the astroglial responses to Aβ was different in monkeys, and monkeys are phylogenetically more similar to humans, monkey cortical and astroglial cultures would be the models of choice to study potential therapeutic applications for humans.

Acknowledgements

The authors thank F. Ono and K. Terao of the Tsukuba Primate Center, National Institute of Infectious Diseases, Japan, for fetal cynomolgus monkey brain samples. This study was supported by a grant-in-aid from the Comprehensive Research on Aging and Health, Ministry of Health, Labor and Welfare, Japan.

References

Behl, C., Davis, J., Cole, G.M., Schubert, D., 1992. Vitamin E protects nerve cells from amyloid β protein toxicity. Biochem. Biophys. Res. Commun. 186, 944–952.

Burdick, D., Soreghan, B., Kwon, M., Kosmoski, J., Knauer, M., Henshen, A., Yates, J., Cotman, C., Glabe, C., 1992. Assembly and aggregation properties of synthetic Alzheimer's A4/beta amyloid peptide analogs. J. Biol. Chem. 267, 546–554.

Cardoso, S.M., Swerdlow, R.H., Oliviera, C.R., 2002. Induction of chytochrome c-mediated apoptosis by amyloid β 25-35 requires functional mitochondria. Brain Res. 931, 117–125.

Citron, M., Westaway, D., Xia, W., Carlson, G., Diehl, T., Levesque, G., Johnson-Wood, K., Lee, M., Seubert, P., Davis, A., Kholodensko, D., Motter, R., Sherrington, R., Perry, B., Yao, H., Strome, R., Lieberburg, I., Rommens, J., Kim, S., Schenk, D., Fraser, P., St. George-Hyslop, P., Selkoe, D.J., 1997. Mutant presenilins of Alzheimer's disease increase production of 42-residue amyloid beta-protein in both transfected cells and transgenic mice. Nature Med. 3, 67–72.

Deb, S., Zhang, J.W., Gottschall, P.E., 2003. β-Amyloid induces the production of active, matrix-degrading proteases in rat cultured rat astrocytes. Brain Res. 970, 205–213.

Funato, H., Yoshimura, M., Yamazaki, T., Saido, T.C., Ito, Y., Yokohujita, J., Okeda, R., Ihara, Y., 1998. Astrocytes containing amyloid beta-protein (Abeta)-positive granules are associated with Abeta40-positive diffuse plaques in the aged human brain. Am. J. Pathol. 152, 983–992.

Glenner, G.G., 1988. Alzheimer's disease: its proteins and genes. Cell 52, 307–308.

Ivins, K.J., Thornton, P.L., Rohn, T.T., Cotman, C.W., 1999. Neuronal apoptosis induced by beta-amyloid is mediated by caspase-8. Neurobiol. Dis. 6, 440–449.

Jarrett, J.T., Berger, E.P., Lansbury Jr., P.T., 1993. The carboxy terminus of the beta amyloid protein is critical for the seeding of amyloid formation: implications for the pathogenesis of Alzheimer's disease. Biochemistry 32, 4693–4697.

Koh, J., Yang, L.L., Cotman, C.W., 1990. β-amyloid protein increase the vulnerability of cultured cortical neurons to excitotoxic damage. Brain Res. 533, 315–320.

LaDu, M.J., Shah, J.A., Reardon, C.A., Getz, G.S., Bu, G., Hu, J., Guo, L., Van Eldik, L.J., 2001. Apolipoprotein E and apolipoprotein E receptors modulate Aβ-induced glial neuroinflammatory responses. Neurochem. Int. 39, 427–434.

Loo, D.T., Copani, A., Pike, C.J., Whittemore, E.R., Walencewicz, A.J., Cotman, C.W., 1993. Apoptosis is induced by β-amyloid in cultured central nervous system neurons. Proc. Natl. Acad. Sci. U.S.A. 90, 7951–7955.

Matsunaga, W., Shirokawa, T., Isobe, K., 2003. Specific uptake of Aβ 1-40 in rat brain occurs in astrocyte, but not in microglia. Neurosci. Lett. 342, 129–131.

Mattson, M.P., Cheng, B., Davis, D., Bryant, K., Lieberburg, I., Rydel, R., 1992. Beta-amyloid peptides destabilize calcium homeostasis and render human cortical neurons vulnerable to excitotoxicity. J. Neurosci. 12, 376–389.

Mattson, M.P., Partin, J., Begley, J.G., 1998. Amyloid beta-peptide induces apoptosis-related events in synapses and dendrites. Brain Res. 807, 167–176.

Morishima, Y., Gotoh, Y., Zieg, J., Barrett, T., Takano, H., Flavell, R., Davis, R.J., Shirasaki, Y., Greenberg, M.E., 2001. β-Amyloid induces neuronal apoptosis via a mechanism that involves the c-Jun n-terminal kinase pathway and the induction of Fas ligand. J. Neurosci. 21, 7551–7560.

Negishi, T., Ishii, Y., Kawamura, S., Kuroda, Y., Yoshikawa, Y., 2002a. Cryopreservation of brain tissue for primary culture. Exp. Anim. 51, 383–390.

Negishi, T., Ishii, Y., Kawamura, S., Kuroda, Y., Yoshikawa, Y., 2002b. Cryopreservation and primary culture of cerebral neurons from cynomolgus monkeys (*Macaca fascicularis*). Neurosci. Lett. 328, 21–24.

Negishi, T., Ishii, Y., Kyuwa, S., Kuroda, Y., Yoshikawa, Y., 2003. Primary culture of cortical neurons, type-1 astrocytes, and microglial cells from cynomolgus monkey (*Macaca fascicularis*) fetuses. J. Neurosci. Method 131, 133–140.

Poirier, J., 1994. Apolipoprotein E in animal models of CNS injury and in Alzheimer's disease. Trends Neurosci. 17, 525–530.

Selkoe, D.J., 1991. The molecular pathology of Alzheimer's disease. Neuron. 6, 487–498.

Smits, H.A., Rijsmus, A., Van Loon, J.H., Wat, J.W.Y., Verhoef, J., Boven, L.A., Nottet, H.S.L.M., 2002. Amyloid-β-induced chemokine production in primary human macrophages and astrocytes. J. Neuroimmnol. 127, 160–168.

Suzuki, N., Cheung, T.T., Cai, X.D., Odaka, A., Otvos Jr., L., Eckman, C., Golde, T.E., Younkin, S.G., 1994. An increased percentage of long amyloid beta protein secreted by familial amyloid beta protein precursor (beta APP717) mutants. Science 264, 1336–1340.

Takashima, A., Honda, T., Yasutake, K., Michel, G., Murayama, O., Murayama, M., Ishiguro, K., Yamaguchi, H., 1998. Activetion of tau protein kinase I/glycogen synthase kinase-3β by amyloid β peptide (25–35) enhances phosphorylation of tau in hippocampal neurons. Neuroscience Res. 31, 317–323.

Troy, C.M., Rabacchi, S.A., Friedman, W.J., Frappier, T.F., Brown, K., Shelanski, M.L., 2000. Caspase-2 mediates neuronal cell death induced by beta-amyloid. J. Neurosci. 20, 1386–1392.

Wyss-Coray, T., Loike, J.D., Brionne, T.C., Lu, E., Anankov, R., Yan, F., Silverstein, S.C., Husemann, J., 2003. Adult mouse astrocytes degrade amyloid-β in vitro and in situ. Nat. Med. 9, 453–457.

Yang, A.J., Chandswangbhuvana, D., Shu, T., Henschen, A., Glabe, C.G., 1999. Intracellular accumulation of insoluble, newly synthesized Aβn-42 in amyloid precursor protein-transfected cells that have been treated with Aβ1-42. J. Biol. Chem. 274 (29), 20650–20656.

Yankner, B.A., Duffy, L.K., Kirschner, D.A., 1990. Neurotrophic and neurotoxic effects of amyloid β protein: reversal by tachykinin neuropeptides. Science 25, 279–282.

Younkin, S.G., 1994. The amyloid beta protein precursor mutations linked to familial Alzheimer's disease alter processing in a way that fosters amyloid deposition. Tohoku J. Exp. Med. 174, 217–223.

Hematopoietic Microchimerism in Sheep After In Utero Transplantation of Cultured Cynomolgus Embryonic Stem Cells

Kyoko Sasaki,[1,6] Yoshikazu Nagao,[2] Yoshihiro Kitano,[3] Hideaki Hasegawa,[1,2] Hiroaki Shibata,[1] Masaaki Takatoku,[4] Satoshi Hayashi,[5] Keiya Ozawa,[4] and Yutaka Hanazono[1,7]

Background. Although directed differentiation of human embryonic stem (ES) cells would enable a ready supply of cells and tissues required for transplantation therapy, the methodology is limited. We have developed a novel method for hematopoietic development from primate ES cells. We first cultured cynomolgus monkey ES cells in vitro and transplanted the cells in vivo into fetal sheep liver, generating sheep with cynomolgus hematopoiesis.

Methods. Cynomolgus ES cells were induced to mesodermal cells on murine stromal OP9 cells with multiple cytokines for 6 days. The cells (average 4.8×10^7 cells) were transplanted into fetal sheep in the liver (n=4) after the first trimester (day 55–73, full term 147 days). The animals were delivered at full term, and two of them were intraperitoneally administered with human stem-cell factor (SCF).

Results. Cynomolgus hematopoietic progenitor cells were detected in bone marrow at a level of 1% to 2% in all four sheep up to 17 months posttransplant. No teratoma was found in the lambs. After SCF administration, the fractions of cynomolgus hematopoiesis increased by several-fold (up to 13%). Cynomolgus cells were also detected in the circulation, albeit at low levels (<0.1%).

Conclusions. Long-term hematopoietic microchimerism from primate ES cells was observed after in vitro differentiation to mesodermal cells, followed by in vivo introduction into the fetal liver microenvironment. The mechanism of such directed differentiation of ES cells remains to be elucidated, but this procedure should allow further investigation.

Keywords: Primate embryonic stem cells, In utero transplantation, Hematopoietic microchimerism, Sheep.

(*Transplantation* 2005;79: 32–37)

A major barrier for most tissue or cellular transplantation therapies is the shortage of donors. Because human embryonic stem (ES) cell lines have dual abilities to proliferate indefinitely and differentiate into multiple tissue cells (*1, 2*), directed differentiation of human ES cells into functionally defied tissue types is a goal in providing an inexhaustible and potentially customized supply of transplantable cells or tissues. Clearly directed differentiation of ES cells is still in its infancy, and the methodology is quite limited. Many researchers have studied in vitro specific differentiation programs through manipulation of the cytokine milieu, cellular microenvironment, and conditional activation of specific gene expression (*3–5*). On the other hand, we and other groups have shown a line of evidence that undifferentiated ES cells respond to local cues after transplantation and differentiate into site-specific cells in rodent and nonhuman primate allogeneic transplantation models (*6, 7*). These studies have highlighted the importance of the in vivo local microenvironment for directed differentiation of ES cells. ES cells can be induced to differentiate into specific cells if exposed to the proper microenvironment. In this study, we have tried to use the in vivo fetal sheep liver microenvironment for hematopoietic development from primate ES cells.

Sheep in utero transplantation has been used as an assay system for human hematopoiesis (*8*). The fetal sheep is immunologically tolerant of allogeneic skin grafts or xenogeneic human hematopoietic cells before 75 days of gestation, which allows avoidance of the immunologic barriers present in postnatal models (*8–10*). In this model, long-term human/sheep hematopoietic chimeras have been established after the transplantation of human hematopoietic stem cells into the fetal sheep at a preimmune stage (*8*). It has also been reported that human mesenchymal stem cells engraft and show site-specific differentiation after in utero transplantation in sheep (*11*).

We have used nonhuman primate (cynomolgus monkey) ES cells (*12*) because this is the most faithful model for human ES cells for generating hematopoietic chimera in sheep. We first cultured cynomolgus ES cells in vitro to differentiate into mesodermal cells and introduced the cells into fetal sheep liver after the first trimester. Fetal liver is a hematopoietic organ at this stage of fetuses. We then examined the in vivo fate of transplanted cell progeny long term.

MATERIALS AND METHODS

Cell Preparation

Cynomolgus macaque ES cells (CMK6) were maintained on a feeder layer of mitomycin C (Kyowa, Tokyo, Japan) treated mouse (BALB/c, Charles River Japan,

This study was supported by the Ministry of Education, Culture, Sports, Science and Technology of Japan.

[1] Division of Regenerative Medicine, Center for Molecular Medicine, Jichi Medical School, Tochigi, Japan.
[2] Department of Agriculture, Utsunomiya University, Tochigi, Japan.
[3] Department of Surgery, National Center for Child Health and Development, Tokyo, Japan.
[4] Division of Hematology, Department of Internal Medicine, Jichi Medical School, Tochigi, Japan.
[5] Department of Obstetrics and Gynecology, National Center for Child Health and Development, Tokyo, Japan.
[6] Department of Plastic and Reconstructive Surgery, Faculty of Medicine, University of Tokyo, Tokyo, Japan.
[7] Address correspondence to: Dr. Yutaka Hanazono, Associate Professor, Head, Division of Regenerative Medicine, Jichi Medical School, 3311–1 Yakushiji, Minamikawachi, Tochigi 329–0498, Japan. E-mail: hanazono@jichi.ac.jp.

Received 3 March 2004. Revision requested 7 April 2004 and 10 June 2004.
Accepted 19 July 2004.

ISSN 0041-1337/05/7901-32
DOI: 10.1097/01.TP.0000144058.87131.C5

Kanagawa, Japan) embryonic fibroblasts, as described previously (*12*). The mouse bone-marrow stromal-cell line OP9 was maintained in α-minimum essential medium (Gibco, Rockville, MD) supplemented with 20% fetal calf serum, as previously described (*13*).

For the in vitro differentiation (induction of hematopoietic differentiation), ES cells were seeded onto mitomycin–C-treated confluent OP9 cell layers in culture dishes in Iscove's modified Dulbecco's medium (Gibco) supplemented with 8% horse serum (Gibco), 8% fetal calf serum, 5×10^{-6} M hydrocortisone (Sigma, St. Lois, MO), and multiple cytokines including 20 ng/mL recombinant human (rh) bone morphogenetic protein-4 (BMP-4; R&D, Minneapolis, MN), 20 ng/mL rh stem-cell factor (SCF, Amgen, Thousand Oaks, CA), 20 ng/mL rh interleukin-3 (Research Diagnostics, Flanders, NJ), 20 ng/mL rh interleukin-6 (Ajinomoto, Osaka, Japan), 20 ng/mL rh vascular endothelial growth factor (VEGF, R&D), 20 ng/mL rh granulocyte colony-stimulating factor (Chugai, Tokyo, Japan), 10 ng/mL rh Flt-3 ligand (Research Diagnostics), and 2 IU/mL rh erythropoietin (Chugai). During differentiation, media were changed every 2 to 3 days. After 6 days of culture, cells were dissociated with 0.25% trypsin (Gibco), collected with a cell scraper, washed with Hanks' balanced salt solution (HBSS, Gibco), resuspended in 0.4 mL of 0.1% bovine serum albumin/HBSS, and used for transplantation. Human cord-blood $CD34^+$ cells used in the present study were obtained at Jichi Medical School Hospital with informed consent.

Transplant Procedures

Pregnant Suffolk ewes (Japan Lamb, Hiroshima, Japan) were bred at the Utsunomiya University Farm. Fetal sheep at 55 to 79 days of gestation (full term 147 days) were used. Before transplantation, ewes were sedated with ketamine (10 mg/kg intramuscularly) and received a 0.5% to 1.0% halothane-oxygen mixture by inhalation by way of an endotracheal tube. The uterus was exposed through a midline laparotomy incision. Donor cells were injected into the fetus in the liver through the uterine wall using a 25-gauge needle under ultrasound guidance. After closure of the abdominal wall, penicillin and streptomycin were administered. The fetus was allowed to come to term. After birth, some lambs were intraperitoneally administered rhSCF at a dosage of 60 μg/kg once a day for 18 or 5 consecutive days.

Hematopoietic Progenitor Assay

To assess cynomolgus hematopoiesis in sheep, clonogenic hematopoietic colonies were produced by growing bone-marrow cells in methylcellulose with defined rh cytokines (Methocult GF+ and MegaCult-C, Stem Cell Technologies, Vancouver, Canada). Bone-marrow cells were aspirated from the iliac bone. From harvested bone-marrow cells, a leukocyte cell fraction was obtained after red–blood-cell lysis with ACK buffer (155 mM NH_4Cl, 10 mM $KHCO_3$ and 0.1 mM EDTA; Wako, Osaka, Japan). Cells were plated in triplicate at 1 to 5×10^4 cells per 35-mm plate. After 14 days, individual colonies were plucked into 50 μL of distilled water and digested with 20 μg/mL proteinase K (Takara, Shiga, Japan) at 55°C for 1 hour, followed by 99°C for 10 minutes. Each sample (5 μL) was used for polymerase chain reaction (PCR) amplification to detect cynomolgus-specific β2-microglobulin gene sequences. Nested PCR was performed. The outer primer set was 5'-GTC TGG ATT TCA TCC ATC TG-3' and 5'- GGC TGT GAC AAA GTC ACA TGG-3', and the inner primer set was 5'-GTC TGG ATT TCA TCC ATC TG-3' and 5'-GGT GAA TTC AGT GTA GTA CAA G-3'. Amplification conditions for both outer and inner PCR were 25 cycles of 94°C for 30 seconds, 58°C for 30 seconds, and 72°C for 30 seconds. Amplified products (135 bp) were resolved on 2% agarose gel and visualized by ethidium bromide staining.

PCR Southern Blotting

Cellular DNA was extracted from peripheral blood and bone-marrow cells after birth and subjected to the cynomolgus-specific β2-microglobulin PCR as described above. The PCR products were resolved on 2% agarose gel and transferred to Hybond-N+ (Amersham, Cleveland, OH). The membrane was hybridized with a radiolabeled cynomolgus-specific β2-microglobulin probe generated by PCR using the following primers: 5'-GTC TGG ATT TCA TCC ATC TG-3' and 5'-GGT GAA TTC AGT GTA GTA CAA G-3'. Radiolabeling of a probe was performed using a DNA labeling kit (Amersham).

RESULTS

In Vitro Culture and In Utero Transplantation

Cynomolgus ES cells were maintained on mouse embryonic fibroblast feeder cells. They form colonies on feeder cells (Fig. 1a). For induction of hematopoietic differentiation, undifferentiated ES cells were placed on murine stromal OP9 cells (*13*) in the presence of multiple cytokines including human BMP-4 and VEGF (*14*). The cell number increased by 10-fold at day 6, and cobblestone-like cells emerged at this time point (Fig. 1b). These cells were negative or only weakly positive for CD34 (hematopoietic) and CD31 (endothelial) markers as assessed by flow cytometry and had little clonogenic hematopoietic colony forming ability in culture (data not shown). These cells likely represent a differentiated population of mesodermal cells. We then transplanted the day-6 ES derivatives (average 4.8×10^7 cells, Table 1) into fetal sheep (n=4) by way of direct injection into the liver under ultrasound guidance after the first trimester (Fig. 1c).

Hematopoietic Microchimerism after Birth

The animals were delivered at full term. Marrow cells were harvested from the iliac bone and plated in methylcellulose. Clonogenic hematopoietic colonies (colony-forming units [CFU]) were thus produced to examine hematopoietic chimerism in the sheep (Fig. 2). Sheep bone-marrow cells generated colonies of clear hematopoietic morphology in this assay. Cynomolgus and sheep cells were equivalent in their colony-formation ability in this culture, and each colony was derived from a single cynomolgus or sheep hematopoietic progenitor cell. Therefore, the ratio of cynomolgus to sheep colony number is considered a chimeric fraction. To distinguish cynomolgus versus sheep colonies, we tried to immunostain colonies with antihuman class I, and more directly hematopoietic-specific antihuman CD45, but they reacted to sheep counterparts or generated a considerable nonspecific staining. We then conducted PCR for monkey-specific β2-microglobu-

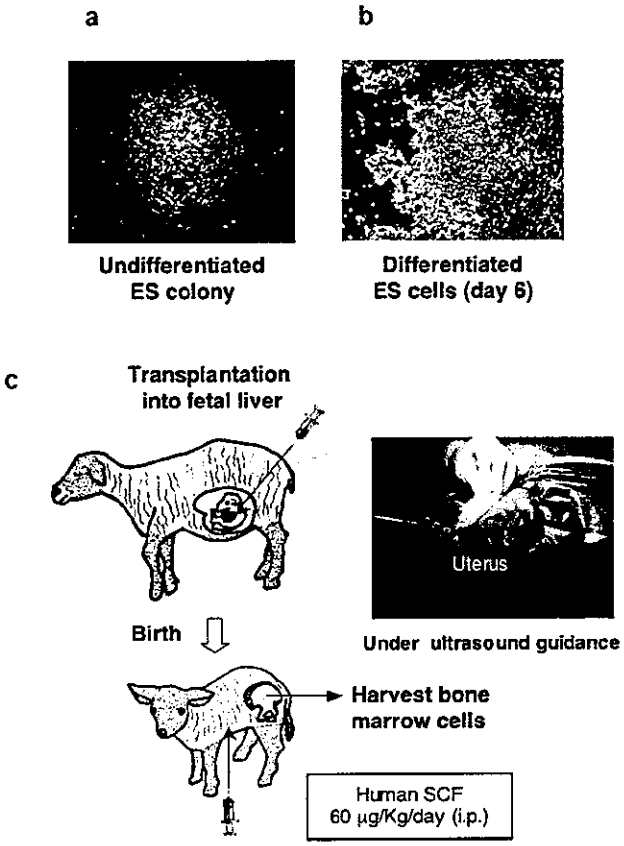

FIGURE 1. In utero transplantation of day 6 cynomolgus embryonic stem (ES)-derived cells. (a) Undifferentiated cynomolgus ES cells were maintained on mouse embryonic fibroblast feeder cells. (b) For hematopoietic induction, undifferentiated ES cells were placed on murine stromal OP9 cells in the presence of multiple cytokines. Cobblestone-like cells emerged at day 6. (c) The day 6 ES derivatives were transplanted directly into the fetal liver after the first trimester. After birth, marrow cells were harvested from the iliac bone and examined for cynomolgus versus sheep hematopoiesis. Some lambs were intraperitoneally (i.p.) administered with human stem-cell factor (SCF) to specifically stimulate cynomolgus hematopoiesis.

lin DNA sequences on DNA isolated from each colony (Fig. 2) (colony PCR). Cynomolgus CFU were clearly detected at a level of 1% to 2% in the bone marrow of all four sheep (Table 1). We repeated colony PCR and confirmed that data were reproducible. We detected both granulocytic and erythroid cynomolgus CFU. Cynomolgus megakaryocytic colonies were not detected, but it was no wonder considering the low frequency of cynomolgus megakaryocytic colony formation in vitro (*15*). The longest follow-up was 17 months after transplantation (14 months after birth), and cynomolgus CFU were still detectable. No lamb developed a teratoma.

Selective Expansion of Cynomolgus Hematopoiesis

To selectively stimulate cynomolgus compared with endogenous hematopoiesis in the sheep, we administered two animals with human SCF, a cytokine that does not cross-react to stimulate sheep hematopoietic progenitors (*16*). A time-course profile of the two animals (No. 141 and No. 182) is shown in Figure 3. In both sheep, in response to the human SCF administration for 18 days, the fractions of cynomolgus CFU increased several-fold (up to 13.2% at day 174 and 4.7% at day 112 posttransplantation, respectively). After cessation of SCF administration, the fractions fell to the original levels. Resumption of human SCF at the same dose but for 5 days produced a similar elevation in the chimeric fractions (up to 4.4% at day 364 and 8.8% at day 187 posttransplantation, respectively). No adverse effects associated with human SCF administration were observed. We did not examine antibody responses to human SCF in the sheep, but this was unlikely to occur because second trials of human SCF administration did work (i.e., increased the chimeric fractions) in both sheep.

Cynomolgus cells were also detected in the circulation, although the fraction was very low (<0.1%), even after human SCF administration as assessed by PCR Southern blotting (Fig. 4). The low levels of cynomolgus cells hampered the lineage analysis by flow cytometry. To detect cynomolgus T lymphocytes in the sheep, we collected the peripheral blood and tried to selectively expand cynomolgus T lymphocytes in the culture with human interleukin-2, antimonkey CD3 (FN-18), and antihuman CD28 (Kolt-2, cross-reacting to monkey CD28) (*17*). However, sheep lymphocytes were also stimulated to expand, and we failed to detect cynomolgus T lymphocytes.

Comparative Study of Repopulating Ability

Next, we transplanted human cord-blood hematopoietic stem cells ($CD34^+$ cells, average 1.8×10^6 cells) into fetal sheep (n=4) instead of day-6 cynomolgus ES derivatives. We used a $CD34^+$ fraction because it was widely used both in sheep in utero transplantation (*18, 19*) and in clinical transplantation of hematopoietic stem cells (*20*), although some investigators used a human $CD34^-$ fraction for sheep in utero transplantation and obtained hematopoietic chimera as well or even better in serial transplantation experiments (*21*). For the present, however, we considered that the $CD34^+$ fraction was an appropriate standard with which to compare the repopulating ability of day-6 cynomolgus ES-derived cells as well. The chimeric fraction in bone-marrow CFU after in utero transplantation of $CD34^+$ cells was 1% to 9% (average 3.7%). Fractions of donor-derived cells in the peripheral blood were also very low (<0.1%) after the transplantation of $CD34^+$ cells. The average cell numbers necessary to achieve 1% chimerism in CFU after birth were estimated to be 4.3×10^7 and 6.0×10^5 for day-6 cynomolgus ES-derived cells and human cord-blood $CD34^+$ cells, respectively.

DISCUSSION

We have generated long-term hematopoietic microchimerism in sheep derived from ES cells. Achieving hematopoietic reconstitution from ES cells has been an enormous challenge. The difficulty is attributable to the developmental immaturity of ES-derived cells, which most closely resemble primitive embryonic yolk-sac hematopoietic progenitors (*22*). The processes governing embryonic versus adult blood formation are distinct, and mouse ES cells do not contribute

TABLE 1. In utero transplantation and donor-cell engraftment in sheep

Transplanted cells	Animals (sex)	In utero transplantation: Transplanted cell number per fetus	In utero transplantation: Gestational day at transplantation (Full term 147 days)	Donor cell-derived CFU in bone marrow* (months posttransplant): After birth	Donor cell-derived CFU in bone marrow* (months posttransplant): After human SCF administration	Average cell number necessary for 1% chimerism
Day 6 ES-derived cells	No. 57 (male)	5.0×10^7	67	1.1% (1/91) at 3.5 months	ND	4.3×10^7
	No. 55 (female)	5.0×10^7	55	1.1% (1/91) at 5 months	ND	
	No. 141 (male)	7.8×10^7	73	1.1% (1/91) at 3 months	13.2% (12/91) at 6 months	
	No. 182 (male)	1.4×10^7	66	1.6% (1/63) at 3 months	8.8% (8/91) at 6 months	
Human cord blood $CD34^+$ cells	No. 71-1 (male)	2.0×10^6	69	8.8% (8/91) at 1 months	ND	6.0×10^5
	No. 71-2 (female)	2.0×10^6	69	4.4% (4/91) at 3.5 months	ND	
	No. 99-1 (male)	1.5×10^6	79	1.1% (1/91) at 1 months	ND	
	No. 99-2 (female)	1.5×10^6	79	4.4% (4/91) at 2 months	ND	

* Percent cynomolgus CFU was calculated by dividing the number of CFU positive for the cynomolgus-specific β2-microglobulin gene sequence by the total number of CFU analyzed.

CFU, colony-forming unit; ND, not done; ES, embryonic stem.

to hematopoietic reconstitution in irradiated mice, unlike stem cells isolated from adult bone marrow (*23, 24*). An effective approach to this obstacle has recently been reported. Genetically engineering mouse ES cells to express a specific transcription factor (HoxB4) or signaling molecule (STAT5) during a specific developmental window has resulted in hematopoietic reconstitution from ES cells in irradiated mice (*5, 25*). However, the requirement for artificial over-expression of those genes is undesirable for clinical applications. Our method to develop hematopoietic engraftment from primate ES cells does not require genetic manipulation, and it is a combination of two steps: in vitro differentiation into mesodermal cells followed by in vivo development into hematopoietic cells in the proper microenvironment of fetal sheep liver.

To examine whether transplanted day-6 ES-derived cells engraft in other tissues, we did one more in utero transplantation experiment using same cultured cynomolgus ES cells (mesodermal cells at day 6) and delivered a fetus at 1 month after transplantation. Although cynomolgus CFU were detected in fetal liver and cord blood, cynomolgus cells were not detectable in any other tissues by a sensitive PCR after the fetal blood was completely washed out (data not shown). Therefore, our method appears to direct the fate of primate ES cells to the hematopoietic lineage.

We assumed that the initial in vitro culture of ES cells into mesodermal cells is crucial for successful engraftment in the fetal liver. In fact, when we transplanted undifferentiated (day 0) cynomolgus ES cells into fetal sheep (n=2), we failed to detect cynomolgus CFU or other nonhematopoietic cells in any fetal tissue at 1 month posttransplantation as assessed by a sensitive PCR (data not shown). Therefore, undifferentiated ES cells do not appear to engraft in fetal sheep, unlike adult mesenchymal or hematopoietic stem cells (*8, 11*), but day-6 ES derivatives (mesodermal cells) can engraft and are susceptible to hematopoietic specification in the fetal-liver microenvironment. For the successful initial in vitro culture of ES cells, there are some points to be noted. First, we used stromal OP9 cells as a feeder. Second, we included BMP-4 and VEGF in the culture medium. The coculture with OP9 and inclusion of BMP-4 and VEGF promote hematopoietic differentiation of ES cells (*13, 14, 26–28*). Finally, we cultured cells in vitro for a relatively short period (6 days) to avoid over-maturation of cells (*14*). The xenogeneic fetal liver is able to provide such cultured ES cells with an adequate microenvironment for support of hematopoietic development (*29*). Factors present in the fetal liver responsible for the development remain to be elucidated.

On the other hand, several issues remain to be further investigated. Although the chimeric fractions increased by several-fold (up to 13%) after SCF administration, the increase was transient. To stably enhance the ES-derived chimeric fraction, an enrichment of cells responsible for the engraftment will be needed before transplantation, as suggested from Table 1 (see average cell numbers necessary to achieve 1% chimerism). Another issue is a very low level of donor-derived cells in the peripheral blood. Ours is quite different from previous human-to-fetal sheep experiments that demonstrated easily detectable peripheral blood chimerism (*16, 19*). This has hampered the lineage analysis of cynomolgus cells in our sheep to obtain further evidence to support hematopoietic differentiation from ES cells. Low levels of pe-

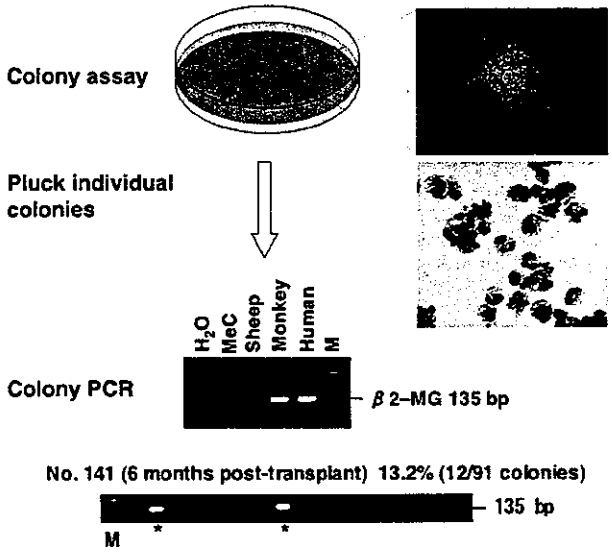

FIGURE 2. Assessment of cynomolgus hematopoiesis in sheep after birth. Bone-marrow cells were harvested from lambs and placed in methylcellulose. Hematopoietic colonies were thus formed. A cytospin specimen (stained with the Wright-Giemsa method) of plucked myeloid colonies demonstrated mature neutrophils. Each colony was derived from a single cynomolgus or sheep hematopoietic progenitor cell. To detect cynomolgus colonies, individual colonies were plucked and examined for cynomolgus-specific β2-microglobulin (β2-MG) sequences by polymerase chain reaction (PCR). PCR products were analyzed on 2% agarose gel. Plucked methylcellulose (MeC) alone (not containing colonies) and sheep colonies generated no bands by the PCR. Colony PCR was repeated at least twice. Representative colony PCR results of sheep No. 141 shown. *Bands positive for the cynomolgus-specific sequence. M, molecular weight marker.

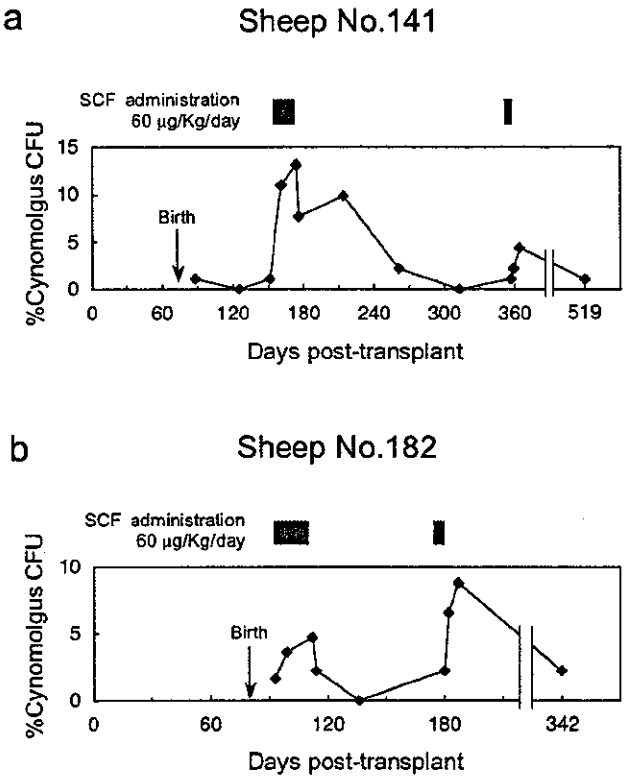

FIGURE 3. Time course of hematopoietic chimerism in the sheep receiving human SCF. (a) In sheep No. 141, human SCF was intraperitoneally administered at 60 μg/kg once a day from day 156 posttransplantation for 18 days. SCF administration was then stopped and tried again from day 352 for 5 days. (b) In sheep No. 182, human SCF was similarly administered from day 94 posttransplantation for 18 days, followed by a second administration at the same dose from day 175 for 5 days. Horizontal axis indicates days after transplantation. Vertical axis shows cynomolgus/sheep chimerism (a ratio of cynomolgus vs. sheep CFU in the bone marrow). Period of human SCF administration (*gray bars*).

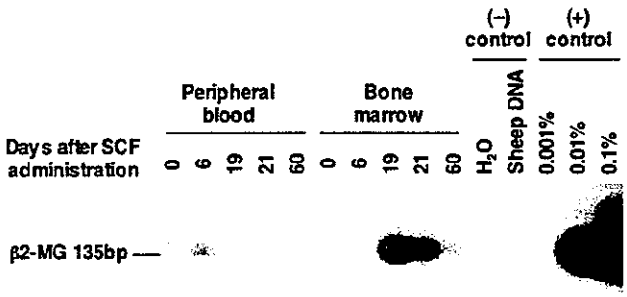

FIGURE 4. Detection of cynomolgus cells in the circulation. DNA was extracted from whole peripheral blood or bone-marrow nucleated cells after birth and subjected to cynomolgus-specific β2-microglobulin (β2-MG) PCR, and Southern blot analysis. Data before and after SCF administration shown. Positive controls show 0.001, 0.01, and 0.1% chimerism (cynomolgus to sheep). Cynomolgus cells were detectable after SCF administration, albeit at low levels (<0.1%).

ripheral chimerism were, however, also found after human $CD34^+$ cells were transplanted in our study. Therefore, the issue is not specific to transplanted ES cells, but is likely to be attributable to the experimental system. A possible explanation may be the different sheep species used in our study (Suffolk versus Dorset Merino). Another possible explanation is immune responses caused by relatively later gestational ages (in the second trimester, day 55–79) at transplantation in our study compared with other recent studies (day 40–45) (*19*). The immune response may have cleared xenogeneic cells from the circulation. The existence of microchimerism does not necessarily guarantee or predict tolerance in other systems (*30, 31*). "The window of opportunity" for successful tolerance induction may be earlier and narrower. To avoid sensitization, transplantation at earlier days may be more efficacious.

In conclusion, long-term hematopoietic microchimerism from primate ES cells is possible after in vitro differentiation to mesodermal cells, followed by in vivo transplantation into the fetal-liver microenvironment. We have used nonhuman primate ES cells in the current study, but if human ES cells are similarly used, human blood cells can be generated in sheep. This procedure should allow for further investigation.

ACKNOWLEDGMENTS

Cynomolgus ES cells were provided by Norio Nakatsuji (Kyoto University, Kyoto, Japan) and Yasushi Kondo (Tanabe Seiyaku Co. Ltd., Osaka, Japan). OP9 cells were provided by Toru Nakano (Osaka University, Osaka, Japan). The authors thank Takayuki Asano, Kyoji Ueda, Yukiko Kishi, and Yujiro Tanaka for help preparing and analyzing samples. The authors are grateful to Cynthia Dunbar for helpful comments on the manuscript. The authors acknowledge Amgen's supply of SCF, Chugai's supply of granulocyte colony-stimulating factor and erythropoietin, and Ajinomoto's supply of interleukin-6.

REFERENCES

1. Thomson JA, Itskovitz-Eldor J, Shapiro SS, et al. Embryonic stem cell lines derived from human blastocysts. *Science* 1998; 282: 1145.
2. Reubinoff BE, Pera MF, Fong C, et al. Embryonic stem cell lines from human blastocysts: somatic differentiation in vitro. *Nat Biotechnol* 2000; 18: 399.
3. Schuldiner M, Yanuka O, Itskovitz-Eldor J, et al. Effects of eight growth factors on the differentiation of cells derived from human embryonic stem cells. *Proc Natl Acad Sci U S A* 2000; 97: 11307.
4. Carpenter MK, Inokuma MS, Denham J, et al. Enrichment of neurons and neural precursors from human embryonic stem cells. *Exp Neurol* 2001; 172: 383.
5. Kyba M, Perlingeiro RC, Daley GQ. HoxB4 confers definitive lymphoid-myeloid engraftment potential on embryonic stem cell and yolk sac hematopoietic progenitors. *Cell* 2002; 109: 29.
6. Bjorklund LM, Sanchez-Pernaute R, Chung S, et al. Embryonic stem cells develop into functional dopaminergic neurons after transplantation in a Parkinson rat model. *Proc Natl Acad Sci U S A* 2002; 99: 2344.
7. Asano T, Ageyama N, Takeuchi K, et al. Engraftment and tumor formation after allogeneic in utero transplantation of primate embryonic stem cells. *Transplantation* 2003; 76: 1061.
8. Zanjani ED, Flake AW, Rice H, et al. Long-term repopulating ability of xenogeneic transplanted human fetal liver hematopoietic stem cells in sheep. *J Clin Invest* 1994; 93: 1051.
9. Silverstein AM, Prendergast RA, Kranerk KL. Fetal response to antigenic stimulus. IV. Rejection of skin homografts by the fetal lamb. *J Exp Med* 1964; 119: 955.
10. Flake AW, Harrison MR, Adzick NS, et al. Transplantation of fetal hematopoietic stem cells in utero: the creation of hematopoietic chimeras. *Science* 1986; 233: 776.
11. Liechty KW, MacKenzie TC, Shaaban AF, et al. Human mesenchymal stem cells engraft and demonstrate site-specific differentiation after in utero transplantation in sheep. *Nat Med* 2000; 6: 1282.
12. Suemori H, Tada T, Torii R, et al. Establishment of embryonic stem cell lines from cynomolgus monkey blastocysts produced by IVF or ICSI. *Dev Dyn* 2001; 222: 273.
13. Nakano T, Kodama H, Honjo T. Generation of lymphohematopoietic cells from embryonic stem cells in culture. *Science* 1994; 265: 1098.
14. Chadwick K, Wang L, Li L, et al. Cytokines and BMP-4 promote hematopoietic differentiation of human embryonic stem cells. *Blood* 2003; 102: 906.
15. Shibata H, Hanazono Y, Ageyama N, et al. Collection and analysis of hematopoietic progenitor cells from cynomolgus macaques (*Macaca fascicularis*): assessment of cross-reacting monoclonal antibodies. *Am J Primatol* 2003; 61: 3.
16. Flake AW, Hendrick MH, Rice HE, et al. Enhancement of human hematopoiesis by mast cell growth factor in human-sheep chimeras created by the in utero transplantation of human fetal hematopoietic cells. *Exp Hematol* 1995; 23: 252.
17. Zhang D, Murakami A, Johnson RP, et al. Optimization of ex vivo activation and expansion of macaque primary CD4-enriched peripheral blood mononuclear cells for use in anti-HIV immunotherapy and gene therapy strategies. *J Acquir Immune Defic Syndr* 2003; 32: 245.
18. Young AJ, Holzgreve W, Dudler L, et al. Engraftment of human cord blood-derived stem cells in preimmune ovine fetuses after ultrasound-guided in utero transplantation. *Am J Obstet Gynecol* 2003; 189: 698.
19. Noia G, Pierelli L, Bonanno G, et al. The intracoelomic route: a new approach for in utero human cord blood stem cell transplantation. *Fetal Diagn Ther* 2004; 19: 13.
20. Berenson RJ, Bensinger WI, Hill RS, et al. Engraftment after infusion of $CD34^+$ marrow cells in patients with breast cancer or neuroblastoma. *Blood* 1991; 77: 1717.
21. Zanjani ED, Almeida-Porada G, Livingston AG, et al. Reversible expression of CD34 by adult human bone marrow long-term engrafting hematopoietic stem cells. *Exp Hematol* 2003; 31: 406.
22. Lu S-J, Li F, Vida L, et al. $CD34^+CD38^-$ hematopoietic precursors derived from human embryonic stem cells exhibit an embryonic gene expression pattern. *Blood* 2004; 103: 4134.
23. Muller AM, Dzierzak EA. ES cells have only a limited lymphopoietic potential after adoptive transfer into mouse recipients. *Development* 1993; 118: 1343.
24. Hole N, Graham GJ, Menzel U, et al. A limited temporal window for the derivation of multilineage repopulating hematopoietic progenitors during embryonal stem cell differentiation in vitro. *Blood* 1996; 88: 1266.
25. Kyba M, Perlingeiro RC, Hoover RR, et al. Enhanced hematopoietic differentiation of embryonic stem cells conditionally expressing Stat5. *Proc Natl Acad Sci U S A* 2003; 100(Suppl 1): 11904.
26. Kaufman DS, Hanson ET, Lewis RL, et al. Hematopoietic colony-forming cells derived from human embryonic stem cells. *Proc Natl Acad Sci U S A* 2001; 98: 10716.
27. Li F, Lu S, Vida L, et al. Bone morphogenetic protein 4 induces efficient hematopoietic differentiation of rhesus monkey embryonic stem cells in vitro. *Blood* 2001; 98: 335.
28. Shalaby F, Ho J, Stanford WL, et al. A requirement for Flk1 in primitive and definitive hematopoiesis and vasculogenesis. *Cell* 1997; 89: 981.
29. Zhang CC, Lodish HF. Insulin-like growth factor 2 expressed in a novel fetal liver cell population is a growth factor for hematopoietic stem cells. *Blood* 2004; 103: 2513.
30. Anderson CC, Matzinger P. Immunity or tolerance: opposite outcomes of microchimerism from skin grafts. *Nat Med* 2001; 7: 80.
31. Gleit ZL, Fuchimoto Y, Yamada K, et al. Variable relationship between chimerism and tolerance after hematopoietic cell transplantation without myelosuppressive conditioning. *Transplantation* 2002; 74: 1535.

Gene Therapy (2005) 12, 203–210

www.nature.com/gt

RESEARCH ARTICLE

Efficient and stable Sendai virus-mediated gene transfer into primate embryonic stem cells with pluripotency preserved

K Sasaki[1,2], M Inoue[3], H Shibata[1], Y Ueda[3], S-i Muramatsu[4], T Okada[1], M Hasegawa[3], K Ozawa[1] and Y Hanazono[1]

[1]*Center for Molecular Medicine, Jichi Medical School, Minamikawachi, Tochigi, Japan;* [2]*Department of Plastic and Reconstructive Surgery, Faculty of Medicine, University of Tokyo, Bunkyo-ku, Tokyo, Japan;* [3]*DNAVEC Corporation, Tsukuba, Ibaraki, Japan; and* [4]*Department of Neurology, Jichi Medical School, Minamikawachi, Tochigi, Japan*

Efficient gene transfer and regulated transgene expression in primate embryonic stem (ES) cells are highly desirable for future applications of the cells. In the present study, we have examined using the nonintegrating Sendai virus (SeV) vector to introduce the green fluorescent protein (GFP) gene into non-human primate cynomolgus ES cells. The GFP gene was vigorously and stably expressed in the cynomolgus ES cells for a year. The cells were able to form fluorescent teratomas when transplanted into immunodeficient mice. They were also able to differentiate into fluorescent embryoid bodies, neurons, and mature blood cells. In addition, the GFP expression levels were reduced dose-dependently by the addition of an anti-RNA virus drug, ribavirin, to the culture. Thus, SeV vector will be a useful tool for efficient gene transfer into primate ES cells and the method of using antiviral drugs should allow further investigation for regulated SeV-mediated gene expression.
Gene Therapy (2005) **12**, 203–210. doi:10.1038/sj.gt.3302409
Published online 14 October 2004

Keywords: *primate embryonic stem cell; Sendai virus vector; gene transfer; green fluorescent protein; pluripotency; ribavirin*

Introduction

Since human embryonic stem (ES) cell lines have the ability to both proliferate indefinitely and differentiate into multiple tissue cells,[1,2] they are expected to have clinical applications as well as to serve as models for basic research and drug development. Although efficient and stable gene transfer into primate ES cells would be useful for such purposes, it has been difficult and only lentiviral vectors have been successful in achieving it.[3–5] We have previously developed Sendai virus (SeV) vectors that replicate in the form of negative-sense single-stranded RNA in the cytoplasm of infected cells and do not go through a DNA phase.[6] SeV vectors can efficiently introduce foreign genes without toxicity into airway epithelial cells,[7] vascular tissue,[8] skeletal muscle,[9] synovial cells,[10] retinal tissue,[11] and hematopoietic progenitor cells.[12] Here we report that the SeV-mediated gene transfer into primate ES cells is very efficient and stable even after the terminal differentiation of the cells. In addition, we show that SeV-mediated transgene expression levels can be reduced by the addition of a ribonucleoside analog, ribavirin, to the culture. Ribavirin is a mutagen and inhibitor of viral RNA polymerase.[13,14] It shows antiviral activity against a variety of RNA viruses and is used to treat infections of hepatitis C virus in combination with interferon-α[15,16] and of lassa fever virus.[17] The method of using antiviral drugs might offer a novel approach for regulated SeV-mediated gene expression in primate ES cells.

Correspondence: Dr Y Hanazono, Center for Molecular Medicine, Jichi Medical School, 3311-1 Yakushiji, Minamikawachi, Tochigi 329-0498, Japan
Received 20 April 2004; accepted 27 August 2004; published online 14 October 2004

Results

SeV-mediated gene transfer into ES cells

In this study, we have used an SeV vector, which is capable of self-replication but incapable of transmitting to other cells.[6] The vector does not encode the fusion (F) protein (Figure 1a), which is essential for viral entry into cells. It can be propagated only in a packaging cell line expressing the F protein. The green fluorescent protein (GFP) gene was introduced after the leader sequence of the vector genome. Cynomolgus ES cells[18] were exposed to the SeV vector for 24 h. Flow cytometric analysis at 2 days after infection showed that 15, 38, and 61% of cells fluoresced at 2, 10, and 50 transducing units (TU) per cell, respectively (Figure 1b). The gene transfer efficiency of about 60% is comparable to or even better than that for lentiviral vectors.[3] We confirmed that the undifferentiated cell fractions remained unchanged after the infection with SeV vector, as assessed by the expression of undifferentiated markers, alkaline phosphatase and SSEA-4 (data not shown). The GFP expression after infection was stable at least for a month. On the other hand, the GFP gene transfer to cynomolgus ES cells with adenovirus- and adeno-associated virus (AAV)-based vectors resulted in much lower expression levels (<20% by flow cytometry) and the levels declined to zero within a week after infection (Figure 1c).

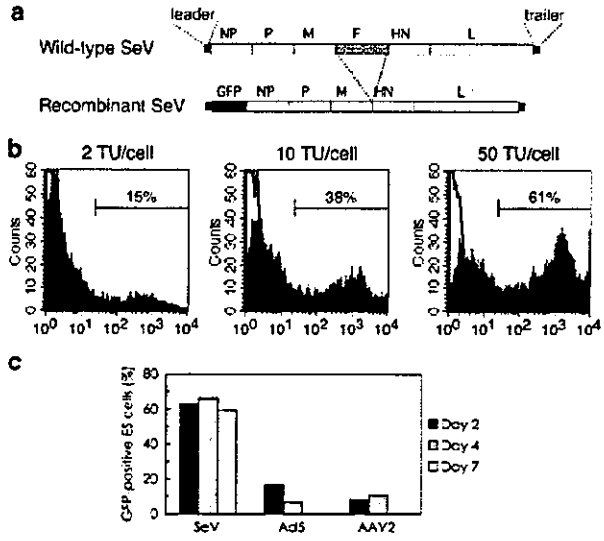

Figure 1 High-level transgene expression in cynomolgus ES cells after infection with SeV vector. (a) Schematic diagrams of the wild-type SeV genome and recombinant F-defective SeV carrying the GFP gene (SeV vector in this study). The SeV genome is 15 384 nucleotides long and its genes (NP, P, M, F, HN, and L) are in order from 3' to 5' in the negative-strand RNA. In the SeV vector, the entire fusion (F) gene was removed and the GFP gene was introduced at a unique NotI site between the leader sequence and NP gene. (b) The GFP expression by the SeV vector in cynomolgus ES cells. Cynomolgus ES cells were infected with the SeV vector at 2, 10, and 50 TU/cell. The flow cytometric profiles at day-2 postinfection are shown in gray. The white areas indicate uninfected ES cells. The fractions of GFP-positive cells are indicated. (c) The GFP expression levels in cynomolgus ES cells infected with the SeV (50 TU/cell), adenovirus serotype 5 (Ad5, 3.4 × 10^2 g.c./cell), and AAV serotype 2 (AAV2, 2.4 × 10^4 g.c./cell) vectors. The fractions of GFP-positive cells were examined by flow cytometry at 2, 4, and 7 days postinfection.

We plucked fluorescent ES cell colonies under a fluorescent microscope once at 1 month after infection and propagated them. After this selection procedure, approximately 90% of the ES cells expressed GFP (Figure 2a and b) and the high-level expression was stable for a year as assessed by flow cytometry (Figure 2c, upper). The mean fluorescence intensity per cell was also stable (Figure 2c, lower), indicating that the replicating vector genome was almost equally delivered to each cell of all progeny. The self-replication of the SeV vector in infected cells was confirmed by RNA-PCR that amplified the viral RNA genomic sequence (Figure 3a). The GFP cDNA sequence, however, could not be detected by DNA-PCR in the infected cells (Figure 3b), indicating that no DNA phase was involved in the GFP expression.

Pluripotency of infected ES cells

The SeV-infected, fluorescent cynomolgus ES cells were able to form fluorescent tumors when transplanted into immunodeficient mice (Figure 4a–c). The fluorescence was observed uniformly by fluorescent microcopy (Figure 4d and e). The tumors consisted of all three embryonic germ layer cells (Figure 4f–i). Thus, the SeV-infected ES cells were capable of forming teratomas and the SeV infection did not spoil the pluripotency of ES cells. The infected, fluorescent cynomolgus ES cells were also able to generate fluorescent embryoid bodies (Figure 5a and b), MAP-2-positive neurons (Figure 5c), clonogenic hematopoietic colonies (Figure 5d and e), and mature functional (NBT test-positive) neutrophils (Figure 5f and g), all of which fluoresced. In addition, the GFP expression levels were not decreased during the teratoma formation or differentiation, indicating that no 'silencing' of the transgene occurred.

Drug-inducible reduction of transgene expression

Next, we examined whether ribavirin inhibits the replication and transcription of the SeV vector resulting in a reduction of transgene expression. We first used a rhesus monkey kidney cell line (LLC-MK2) to test the effect of ribavirin on the replication and transcription of the SeV vector. LLC-MK2 is a standard control cell line for SeV infection. Ribavirin was added at various concentrations 2 days after the infection. The formation of viral particles quantified by the hemagglutination assay decreased drastically upon the addition of ribavirin (Figure 6a). The decrease was dependent on the dose of ribavirin. The GFP expression was also depressed dose-dependently (Figure 6b). Thus, ribavirin dose-dependently inhibits the replication and transcription of the SeV vector in LLC-MK2 cells. The toxicity associated with ribavirin was not observed in LLC-MK2 cells.

We then examined the effect of ribavirin on SeV-infected, fluorescent cynomolgus ES cells. The addition of ribavirin also resulted in a dose-dependent reduction of GFP expression in the cells (Figure 6c). Although the GFP expression was almost completely inhibited after a 3-day exposure with 4 mM of ribavirin, the cells could not be propagated thereafter. Ribavirin at high concentrations (>1 mM) hampered the proliferation of cynomolgus ES cells. With lower concentrations (0.5–0.75 mM) of ribavirin, the GFP expression level decreased by half. After the discontinuation of ribavirin treatment, the cells could be propagated and nearly regained the original level of GFP expression. The undifferentiated cell fractions were unchanged after the discontinuation as assessed by alkaline phosphatase and SSEA-4 staining (Figure 6d).

Discussion

There are several advantages in using SeV vectors over other vectors. (i) SeV vectors can infect nondividing, quiescent cells as well as dividing cells unlike oncoretroviral vectors.[7–11] Thus, they can be used to infect cells that are terminally differentiated as well as at various stages of differentiation, whether they are dividing or not. (ii) SeV vector-mediated gene transfer does not require a DNA phase. Thus, there is no concern about the unwanted integration of foreign sequences into the host genome unlike with oncoretroviral or lentiviral vectors. (iii) Transgene expression is stable even in dividing cells since the SeV vector replicates by itself in the cytoplasm of host cells. On the other hand, gene transfer using nonreplicating adenoviral and AAV vectors resulted in decreased levels of transgene expression in dividing cells over time, since the non-replicating transgene was

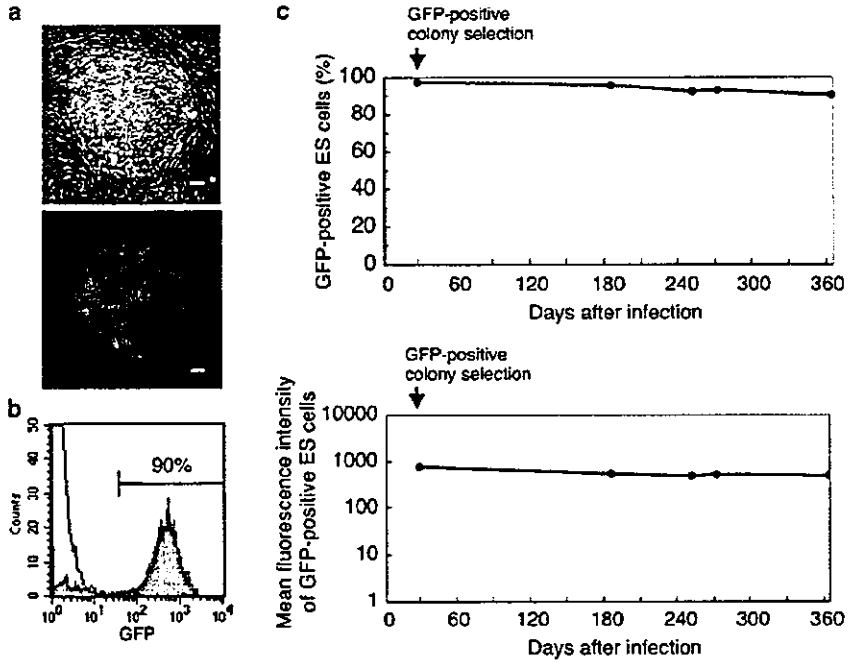

Figure 2 Stable SeV-mediated transgene expression in cynomolgus ES cells. Fluorescent ES cell colonies were plucked under a fluorescent microscope once at 1 month after infection and the cells were further propagated. (a) Phase-contrast (upper) and fluorescence (lower) images of a cynomolgus ES cell colony at day 370 after infection. Bar = 100 μm. (b) Flow cytometric analysis of SeV-infected cynomolgus ES cells at day 370 after infection (shown in green). The percentage of GFP-positive cells is indicated. Uninfected, parental cynomolgus ES cells are indicated by another line (white area). (c) The percentage of GFP-positive cells (upper) and mean fluorescence intensity per GFP-positive cell (lower) after infection with the SeV vector at 10 TU/cell are shown as a function of time (days).

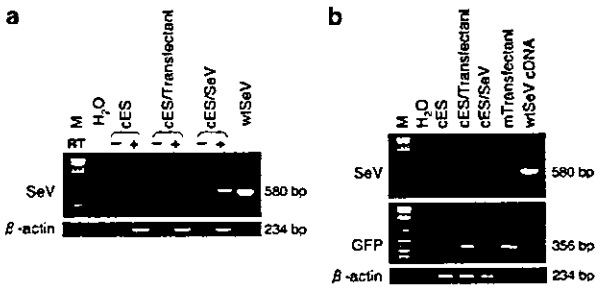

Figure 3 DNA-independent replication and transcription of SeV vector. Total cellular RNA and DNA were extracted from cynomolgus ES cells at day 284 after infection with the SeV vector. RNA-PCR (a) and DNA-PCR (b) for the SeV RNA genome or GFP sequence were conducted. The cynomolgus β-actin sequence was used as an internal control. In the RNA-PCR (a), negative results obtained without reverse transcriptase (designated RT−) confirmed that the amplified products were not derived from cellular DNA. M, 100-kb DNA ladder; cES, naive cynomolgus ES cells; cES/Transfectant, cynomolgus ES cells stably expressing the GFP gene after transfection,[33] cES/SeV, cynomolgus ES cells infected with the SeV vector; wtSeV, wild-type SeV genome; mTransfectant, a GFP-positive mouse cell line after transfection.

diluted out. (iv) The SeV vector is much less unlikely to generate wild-type virus *in vitro* or *in vivo* than oncoretroviral and lentiviral vectors, since homologous recombination between RNA genomes is very rare indeed in negative-strand RNA viruses.[19] (v) The SeV genome is not subject to cellular epigenetic modifications such as methylation, and thus it is unlikely that methylation-based silencing of transgene expression occurs.

No cytotoxic or differentiating effect on ES cells associated with the SeV infection was observed in our study. However, the wild-type SeV contains immunogenic surface proteins, hemagglutinin-neuraminidase (HN) and F proteins, which potentially induce antibody responses.[20,21] For future clinical applications, it would be desired that as many viral genes as possible are deleted from the vector backbone to permit reapplication, improve the safety, and lessen the possible toxicity of SeV vectors. To this end, we have developed a series of attenuated SeV vectors that are F gene-deleted,[6] F gene-deleted with preferable mutations,[22] M gene-deleted,[23] or have deletions of both F and M genes.[24] The modified vectors would be safer for *in vivo* use.

Ribavirin at high concentrations seems toxic to ES cells; presumably, it directly hampers viability and proliferation potential of ES cells. However, we cannot tell whether the observed toxicity is simply due to its toxicity to ES cells, as feeder cells are more highly sensitive to ribavirin than ES cells. In fact, while feeder cells died at 1 mM of ribavirin, cocultured ES cells were alive at this concentration for some time. Cynomolgus ES cells lose pluripotency and proliferation potential without feeder cells. Thus, the observed toxicity to ES cells may also be a secondary event following the injury of feeder cells. Whether the cytotoxicity is primary or secondary, it will be necessary to find modified compounds of less cytotoxicity.

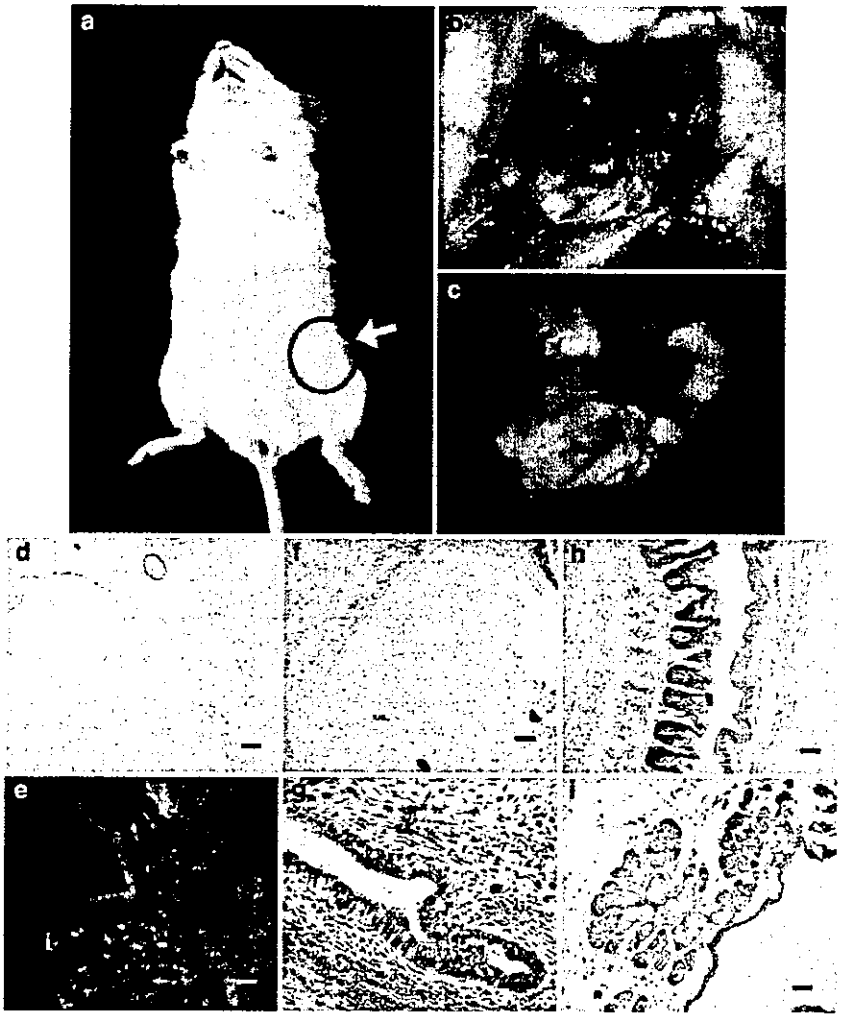

Figure 4 Pluripotency of SeV-infected cynomlgus ES cells. Tumors formed in NOD-SCID mice after inoculation of the SeV-infected cynomolgus ES cells (a). The tumor was fluorescing ((b), bright field; (c), dark field). Fluorescence was observed uniformly in the tumor under a fluorescent microscope ((d), bright field; (e), dark field). The tumor contained all three embryonic germ layer cells; cartilage (f), ciliated columnar epithelium (g), skin (h), and sebaceous gland (i) (stained with hematoxylin and eosin). Bar = 100 μm.

Materials and methods

Cell culture

Cynomolgus ES cells (CMK6) were maintained on a feeder layer of mitomycin C (Kyowa, Tokyo, Japan)-treated mouse (BALB/c) embryonic fibroblasts as described previously.[18] The culture medium consisted of Dulbecco's modified Eagle's medium (DMEM)/F12 (Invitrogen, Carlsbad, CA, USA) supplemented with 15% ES cell-qualified fetal calf serum (FCS; Invitrogen), 0.1 mM 2-mercaptoethanol (Sigma, St Louis, MO, USA), 2 mM glutamine (Invitrogen), 0.1 mM nonessential amino acids (Invitrogen), and antibiotics (100 U/ml penicillin and 100 μg/ml streptomycin, Irvine Scientific, Santa Ana, CA, USA). The ES cell colonies were routinely passaged every 3–4 days after dissociation with a combined approach of 0.25% trypsin (Invitrogen) digestion and mechanical cutting. Alkaline phosphatase staining was conducted with an Alkaline Phosphatase Chromogen Kit (Biomeda, Foster City, CA, USA). Embryoid bodies were produced by culturing ES cell aggregates in Petri dishes. LLC-MK2 cells (1×10^6) were grown in six-well plates and cultured in Eagle's minimal essential medium (Invitrogen) supplemented with 10% FCS.

Vectors

The F-defective SeV vector carrying the GFP gene was constructed as previously described.[6] The vector titer was 1.8×10^9 TU/ml determined by counting fluorescent cells after the infection of LLC-MK2 cells. Gene transfer was conducted by adding various concentrations of the SeV vector solution to culture media. After 24 h of incubation, the cells were washed twice with phosphate-buffered saline (PBS) and fresh medium was added. In some experiments, ribavirin (1-β-D-ribofuranosyl-1,2,4-triazole-3-carboxamide; Sigma) was added at various concentrations to the culture media after infection. The

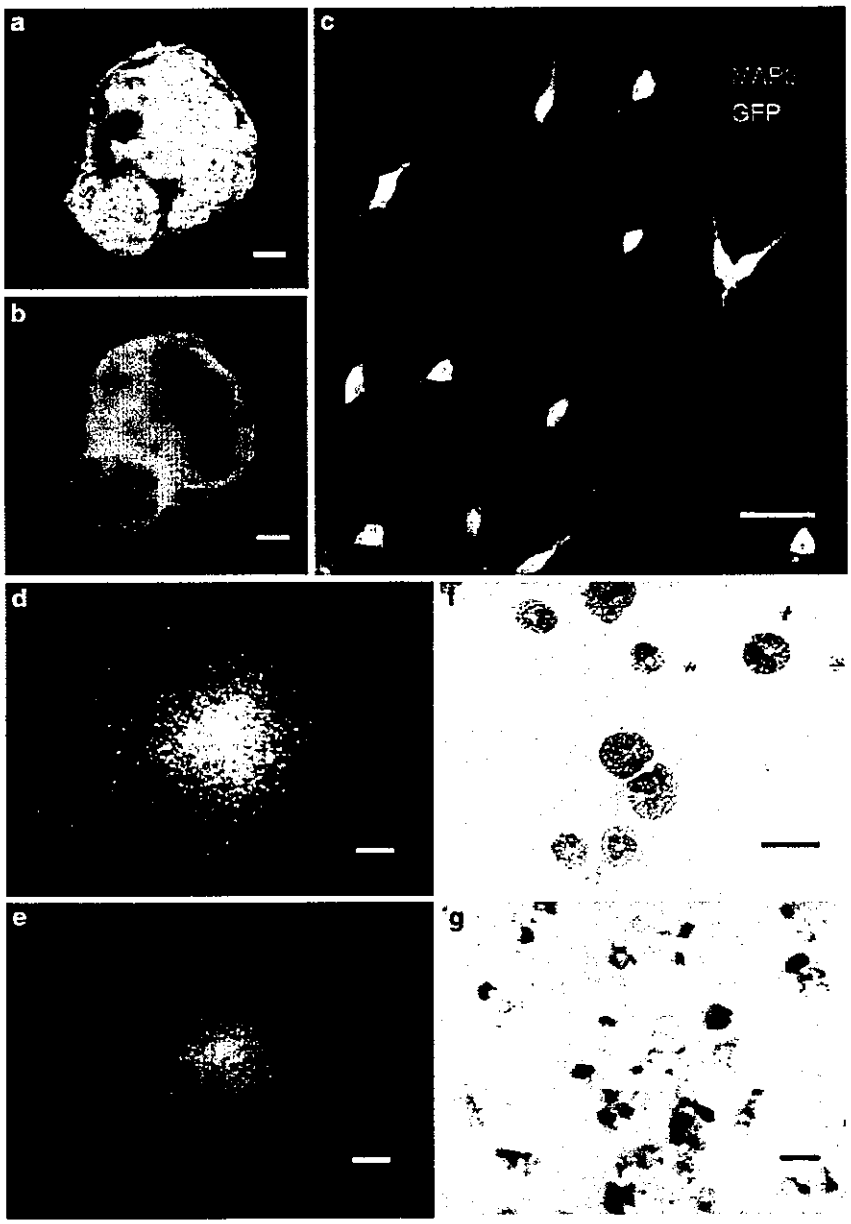

Figure 5 Stable transgene expression during differentiation. A day-20 cystic embryoid body was observed under a fluorescent phase-contrast microscope, confirming that the embryoid body was fluorescing ((a), bright field; (b), dark field). After infection with the SeV vector, fluorescent cynomolgus ES cells differentiated into neural cells. Double immunostaining with anti-GFP (green) and ant-MAP-2 (red) confirmed that differentiated neural cells expressed GFP (c). Yellow cells indicate GFP-expressing neurons. SeV-infected, fluorescent cynomolgus ES cells also differentiated into fluorescent hematopoietic cells. A clonogenic hematopoietic colony was fluorescing ((d) bright field; (e), dark field). A cytospin specimen of hematopoietic colony cells (Wright–Giemsa staining) showed that the cells were mature granulocytes (f). The infected ES cell-derived, fluorescent neutrophils were positive for NBT (stained in black (g)). Bar = 100 μm (a, b, g); 50 μm (c, f); 500 μm (d, e).

viral particles in infected cells were quantified by a hemagglutination assay as described previously.[25]

An adenovirus serotype 5-based vector carrying the GFP gene was constructed as reported.[26] It contained the cytomegalovirus (CMV) promoter, simian virus (SV)-40 intron, and SV-40 polyadenylation signal. An AAV serotype 2-based vector expressing the GFP gene under the control of the chicken β-actin promoter with the CMV immediate-early enhancer (a gift from Dr J Miyazaki) was prepared as described previously.[27] Gene transfer experiments were performed using 3.4×10^2 genome copies (g.c.)/cell of the adenoviral vector or 2.4×10^4 g.c./cell of the AAV vector. The period of exposure was 48 h.

Flow cytometry

GFP and SSEA-4 expression was analyzed on a FACScan (Becton Dickinson, Franklin Lakes, NJ, USA) using the

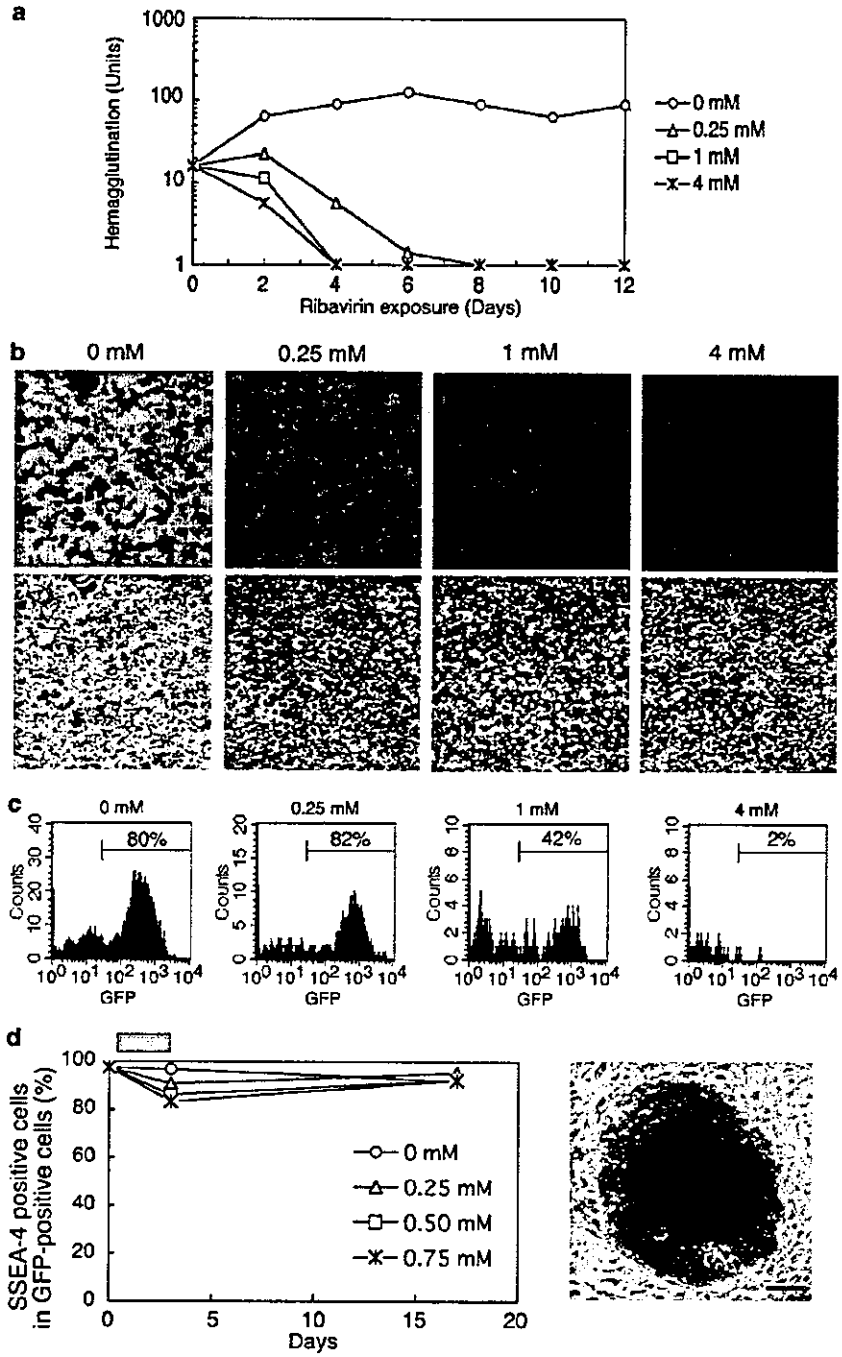

Figure 6 Ribavirin-regulated transgene expression. (a) A rhesus kidney cell line (LLC-MK2) was infected with the SeV vector at 3 TU/cell. Ribavirin was started at various concentrations on day 2 after the infection. The formation of viral particles in the infected LLC-MK2 cells was examined by the hemagglutination assay. (b) The ribavirin-treated LLC-MK2 cells were observed under a fluorescent microscope after an 8-day exposure of ribavirin (upper, dark field; lower, bright field). (c) Ribavirin was added at various concentrations to the SeV-infected, fluorescent cynomolgus ES cells. The GFP expression was assessed by flow cytometry after a 3-day exposure of ribavirin. (d) The fractions of SSEA-4-positive ES cells were assessed by flow cytometry with anti-SSEA-4 before and after a 3-day exposure of ribavirin and are shown as a function of time (days) in the left panel. A gray bar indicates ribavirin treatment. ES cells were stained for alkaline phosphatase (in red) at day 21 after a 3-day exposure of 0.75 mM ribavirin and are shown in the right panel. Bar = 100 μm.

CellQuest software (Becton Dickinson). For SSEA-4 staining, cells were incubated with a primary antibody, anti-SSEA-4 (MC-813-70; Chemicon, Temecula, CA, USA), and then a secondary antibody, PE-conjugated F(ab')2 fragment of rabbit anti-mouse immunoglobulins (DakoCytomation, Glostrup, Denmark). Cocultured BALB/c feeder cells could be distinguished from cynomolgus ES cells by using PE-conjugated anti-mouse

H-2d (SF1-1.1; PharMingen, San Diego, CA, USA), which does not react to cynomolgus cells but does react to BALB/c cells.

Teratoma formation

Cynomolgus ES cells (approximately 10^6 cells per site) were injected subcutaneously into the hind leg of 6- to 8-week-old nonobese diabetic/severe combined immunodeficient mice (Jackson Laboratory, Bar Harbor, ME, USA). The resulting tumors (usually 9–12 weeks after the injection) were dissected and fixed in 4% paraformaldehyde. For histological analysis, samples from the tumors were embedded in paraffin and stained with hematoxylin and eosin. To observe GFP fluorescence, samples were embedded in OTC compound (Sakura, Zoeterwoude, Netherlands), frozen, sectioned, and examined under a fluorescence microscope.

Hematopoietic differentiation

The mouse bone marrow stromal cell line OP9 was maintained in α-modified minimum essential medium (Invitrogen) supplemented with 20% FCS as described previously.[28] For induction of hematopoietic differentiation, ES cells were seeded onto a mitomycin C-treated confluent OP9 cell layer in six-well plates. Medium to support the differentiation was described elsewhere.[29] Cells at day 18 were placed in Methocult GF+ media (StemCell Technologies, Vancouver, Canada) at 1×10^4 and 1×10^5 cells per plate and clonogenic hematopoietic colonies were produced. After 14 days, individual colonies were removed and spun onto glass slides. Cells were stained with the Wright–Giemsa method. The nitro blue tetrazolium (NBT, Sigma) reduction test was performed on the cells as a granulocyte functional assay according to a previously described method.[30]

Neural differentiation

The induction of neural differentiation was carried out as described previously.[31] Day-4 embryoid bodies were plated onto tissue culture dishes and nestin-positive cells were selected in DMEM/F12 medium supplemented with 5 μg/ml of insulin (Sigma), 50 μg/ml of transferrin (Sigma), 30 nM selenium chloride (Sigma), and 5 μg/ml of fibronectin (Sigma) for 5 days. Cells were then trypsinized and plated in polyornithine-coated dishes (15 μg/ml) and expanded in N2 medium[32] supplemented with 1 μg/ml of laminin (Sigma) and 10 μg/ml of basic fibroblast growth factor (bFGF; Roche, Basel, Switzerland) for 6 days. Differentiation was induced by removal of bFGF. To confirm the neural differentiation, cells were stained with anti-human MAP-2. Briefly, cells were fixed in 4% paraformaldehyde in PBS and incubated with anti-human MAP-2 (HM-2; Sigma; diluted 1:4000) and then by Alexa Fluor 594-labeled antibody (diluted 1:500; Molecular Probe, Eugene, OR, USA). The samples were examined under a fluorescence microscope.

DNA-PCR

DNA-PCR for the SeV genome and GFP sequences was carried out as follows. DNA was extracted using the QIAamp DNA mini kits (Qiagen, Hilden, Germany) and 250 ng was used for each PCR with ExTaq (Takara, Shiga, Japan). Amplification conditions were 30 cycles of 94°C for 1 min, a variable annealing temperature (noted below) for 1 min, and 72°C for 1 min. The amplified products were run on 2% agarose gel and visualized by ethidium bromide staining. Primer sequences, annealing temperatures and product sizes were as follows: the SeV vector genome sequence: 5′-AGA GAA CAA GAC TAA GGC TAC C-3′ and 5′-ACC TTG ACA ATC CTG ATG TGG-3′ (55°C, 580 bp); the GFP sequence: 5′-CGT CCA GGA GCG CAC CAT CTT C-3′ and 5′-GGT CTT TGC TCA GGG CGG ACT-3′ (60°C, 356 bp). the cynomolgus β-actin sequence: 5′-CAT TGT CAT GGA CTC TGG CGA CGG-3′ and 5′-CAT CTC CTG CTC GAA GTC TAG GGC-3′ (60°C, 234 bp).

RNA-PCR

RNA-PCR for the SeV RNA genomic sequence was carried out as follows. Total RNA was extracted using RNA STAT-60 (Tel-Test, Friendswood, TX, USA). Reverse transcription was conducted by using Taqman reverse transcription reagents (Applied Biosystems, Foster City, CA, USA). The product (250 ng) after the reverse transcription was used for the subsequent PCR as described above.

Acknowledgements

Cynomolgus ES cells were provided by Norio Nakatsuji (Kyoto University, Kyoto, Japan), Yasushi Kondo (Tanabe Seiyaku Co. Ltd, Osaka, Japan), and Ryuzo Torii (Shiga University of Medical Science, Shiga, Japan). OP9 cells were provided by Toru Nakano (Osaka University, Osaka, Japan). We thank Yujiro Tanaka and Takayuki Asano for cultivating cynomolgus ES cells and Takeshi Hara for conducting NBT tests. We also thank Natsuko Kurosawa for technical assistance.

References

1 Thomson JA *et al.* Embryonic stem cell lines derived from human blastocysts. *Science* 1998; **282**: 1145–1147.
2 Reubinoff BE *et al.* Embryonic stem cell lines from human blastocysts: somatic differentiation *in vitro*. *Nat Biotechnol* 2000; **18**: 399–404.
3 Asano T *et al.* Highly Efficient gene transfer into primate embryonic stem cells with a simian lentivirus vector. *Mol Ther* 2002; **6**: 162–168.
4 Ma Y *et al.* High-level sustained transgene expression in human embryonic stem cells using lentiviral vectors. *Stem Cells* 2003; **21**: 111–117.
5 Gropp M *et al.* Stable genetic modification of human embryonic stem cells by lentiviral vectors. *Mol Ther* 2003; **7**: 281–287.
6 Li HO *et al.* A cytoplasmic RNA vector derived from nontransmissible Sendai virus with efficient gene transfer and expression. *J Virol* 2000; **74**: 6564–6569.
7 Yonemitsu Y *et al.* Efficient gene transfer to airway epithelium using recombinant Sendai virus. *Nat Biotechnol* 2000; **18**: 970–973.
8 Masaki I *et al.* Recombinant Sendai virus-mediated gene transfer to vasculature: a new class of efficient gene transfer vector to the vascular system. *FASEB J* 2001; **15**: 1294–1296.
9 Shiotani A *et al.* Skeletal muscle regeneration after insulin-like growth factor I gene transfer by recombinant Sendai virus vector. *Gene Therapy* 2001; **8**: 1043–1050.
10 Yamashita A *et al.* Fibroblast growth factor-2 determines severity of joint disease in adjuvant-induced arthritis in rats. *J Immunol* 2002; **168**: 450–457.

11 Ikeda Y *et al.* Recombinant Sendai virus-mediated gene transfer into adult rat retinal tissue: efficient gene transfer by brief exposure. *Exp Eye Res* 2002; **75**: 39–48.
12 Jin CH *et al.* Recombinant Sendai virus provides a highly efficient gene transfer into human cord blood-derived hematopoietic stem cells. *Gene Therapy* 2003; **10**: 272–277.
13 Crotty S *et al.* The broad-spectrum antiviral ribonucleoside ribavirin is an RNA virus mutagen. *Nat Med* 2000; **6**: 1375–1379.
14 Vo NV, Young KC, Lai MM. Mutagenic and inhibitory effects of ribavirin on hepatitis C virus RNA polymerase. *Biochemistry* 2003; **42**: 10462–10471.
15 McHutchison JG *et al.* Interferon alfa-2b alone or in combination with ribavirin as initial treatment for chronic hepatitis C. Hepatitis Interventional Therapy Group. *N Engl J Med* 1998; **339**: 1485–1492.
16 Davis GL *et al.* Interferon alfa-2b alone or in combination with ribavirin for the treatment of relapse of chronic hepatitis C. International Hepatitis Interventional Therapy Group. *N Engl J Med* 1998; **339**: 1493–1499.
17 McCormick JB *et al.* Lassa fever. Effective therapy with ribavirin. *N Engl J Med* 1986; **314**: 20–26.
18 Suemori H *et al.* Establishment of embryonic stem cell lines from cynomolgus monkey blastocysts produced by IVF or ICSI. *Dev Dyn* 2001; **222**: 273–279.
19 Spann KM, Collins PL, Teng MN. Genetic recombination during coinfection of two mutants of human respiratory syncytial virus. *J Virol* 2003; **77**: 11201–11211.
20 Tozawa H *et al.* Neutralizing activity of the antibodies against two kinds of envelope glycoproteins of Sendai virus. *Arch Virol* 1986; **91**: 145–161.
21 Tashiro M, Tobita K, Seto JT, Rott R. Comparison of protective effects of serum antibody on respiratory and systemic infection of Sendai virus in mice. *Arch Virol* 1989; **107**: 85–96.
22 Inoue M *et al.* Nontransmissible virus-like particle formation by F-deficient Sendai virus is temperature sensitive and reduced by mutations in M and HN proteins. *J Virol* 2003; **77**: 3238–3246.
23 Inoue M *et al.* A new Sendai virus vector deficient in the matrix gene does not form virus particles and shows extensive cell-to-cell spreading. *J Virol* 2003; **77**: 6419–6429.
24 Inoue M *et al.* Recombinant Sendai virus vectors deleted in both the matrix and the fusion genes: efficient gene transfer with preferable properties. *J Gene Med*, published online 5 May 2004. doi:10.1002/jgm.597.
25 Kato A *et al.* Initiation of Sendai virus multiplication from transfected cDNA or RNA with negative or positive sense. *Genes Cells* 1996; **1**: 569–579.
26 Okada T *et al.* Efficient directional cloning of recombinant adenovirus vectors using DNA–protein complex. *Nucleic Acids Res* 1998; **26**: 1947–1950.
27 Okada T *et al.* Adeno-associated viral vector-mediated gene therapy of ischemia-induced neuronal death. *Methods Enzymol* 2002; **346**: 378–393.
28 Nakano T, Kodama H, Honjo T. Generation of lympho-hematopoietic cells from embryonic stem cells in culture. *Science* 1994; **265**: 1098–1101.
29 Li F *et al.* Bone morphogenetic protein 4 induces efficient hematopoietic differentiation of rhesus monkey embryonic stem cells *in vitro*. *Blood* 2001; **98**: 335–342.
30 Sekhsaria S *et al.* Peripheral blood progenitors as a target for genetic correction of $p47^{phox}$-deficient chronic granulomatous disease. *Proc Natl Acad Sci USA* 1993; **90**: 7446–7450.
31 Lee SH *et al.* Efficient generation of midbrain and hindbrain neurons from mouse embryonic stem cells. *Nat Biotechnol* 2000; **18**: 675–679.
32 Johe KK *et al.* Single factors direct the differentiation of stem cells from the fetal and adult central nervous system. *Genes Dev* 1996; **10**: 3129–3140.
33 Takada T *et al.* Monkey embryonic stem cell lines expressing green fluorescent protein. *Cell Transplant* 2002; **11**: 631–635.

THE JOURNAL OF GENE MEDICINE
J Gene Med 2003; 5: 921–928.
Published online 20 June 2003 in Wiley InterScience (www.interscience.wiley.com). DOI: 10.1002/jgm.431

RESEARCH ARTICLE

Efficient gene transfer of a simian immunodeficiency viral vector into cardiomyocytes derived from primate embryonic stem cells

Mihoko Nagata,[1] Masafumi Takahashi,[2,4]* Shin-ichi Muramatsu,[1]* Yasuji Ueda,[7] Yutaka Hanazono,[5] Koichi Takeuchi,[6] Koji Okada,[3] Yutaka Suzuki,[8] Yasushi Kondo,[8] Masafumi Suemori,[9] Uichi Ikeda,[2] Imaharu Nakano,[1] Eiji Kobayashi,[4] Mamoru Hasegawa,[7] Keiya Ozawa,[5] Norio Nakatsuji[9,10] and Kazuyuki Shimada[2]

[1]*Division of Neurology, Department of Medicine, Jichi Medical School, Tochigi 329-0498, Japan;* [2]*Division of Cardiology, Department of Medicine, Jichi Medical School, Tochigi 329-0498, Japan;* [3]*Division of Endocrinology, Department of Medicine, Jichi Medical School, Tochigi 329-0498, Japan;* [4]*Division of Organ Replacement Research, Center for Molecular Medicine, Jichi Medical School, Tochigi 329-0498, Japan;* [5]*Division of Genetic Therapeutics, Center for Molecular Medicine, Jichi Medical School, Tochigi 329-0498, Japan;* [6]*Department of Anatomy, Jichi Medical School, Tochigi 329-0498, Japan;* [7]*DNAVEC Research, Inc., Ibaraki 305-0856, Japan;* [8]*Tanabe Seiyaku Co., Ltd., Osaka 532-8505, Japan;* [9]*Department of Development and Differentiation, Institute for Frontier Medical Sciences, Kyoto University, Kyoto 606-8507, Japan;* [10]*Stem Cell Research Center, Institute for Frontier Medical Sciences, Kyoto University, Kyoto 606-8507, Japan*

*Correspondence to: Masafumi Takahashi or Shin-ichi Muramatsu, Division of Organ Replacement Research or Division of Neurology, Jichi Medical School, Minamikawachi-machi, Tochigi 329-0498, Japan. E-mail: masafumi@jichi.ac.jp or muramats@jichi.ac.jp

Received: 18 December 2002
Revised: 7 April 2003
Accepted: 5 May 2003

Abstract

Background Embryonic stem (ES) cells continually proliferate and can generate large numbers of differentiated cells. Genetic manipulation of transplantable cells derived from primate ES cells offers considerable potential for development research and regenerative cell therapy. However, protocols for efficient gene transfer into primate ES-cell-derived cells have not yet been established.

Methods Spontaneously contracting areas were derived from cynomolgus monkey ES cells. Features of cardiomyocytes in the area were analyzed according to gene expression (RT-PCR), morphology (immunostaining and electron microscopy), and function (intracellular calcium transience). Beating cells were transduced using a simian immunodeficiency virus (SIV) vector expressing enhanced green fluorescence protein (EGFP), then transplanted into ischemic rat myocardium.

Results Beating cells derived from monkey ES cells displayed gene expression, ultrastructural and functional properties of early-stage cardiomyocytes. Highly efficient (97% cardiac phenotype) and stable transduction of these ES-cell-derived cardiomyocytes was achieved using SIV vector without altering contractile function. In addition, transduced cardiomyocytes survived in the myocardium of a rat myocardial infarction model.

Conclusions A lentiviral vector system based on SIV represents a useful vehicle for genetic modification of cardiomyocytes derived from primate ES cells, and can extend the application of primate ES cells to gene therapy.

Keywords embryonic stem cell; cardiomyocyte; simian immunodeficiency virus; cell transplantation; myocardial infarction

Introduction

The generation of various differentiated cells from pluripotent embryonic stem (ES) cells provides a renewable resource not only for studying the mechanism of early development *in vitro*, but also for cell transplantation therapy. Among many specialized cells in adults, cardiomyocytes are terminally differentiated and have no or only limited regenerative capacity after injury such as myocardial infarction [1]. Thus, the transplantation of functional cardiomyocytes into the damaged myocardium would have therapeutic potential. Recent studies have demonstrated that human ES cells can differentiate into cardiomyocytes with structural and functional properties *in vitro* [2–5]. Although human ES cells hold promise for clinical applications, an alternative model system based on ES cells derived from

experimental animals may be necessary for pre-clinical studies, including allogenic transplantation. We established cynomolgus monkey (*Macaca fascicularis*) ES cell lines [6] that are similar to human ES cells but distinct from murine ES cells in terms of morphology, expression of surface markers, feeder- and leukemia inhibitory factor-dependence and other factors. These features indicate that cynomolgus ES cells represent a suitable pre-clinical model for cell transplantation therapy.

Gene transfer into transplantable cells has potential to enhance the effects of cell replacement therapy. Although murine ES cells can be transduced by electroporation or mouse stem cell virus (MSCV)-based retroviral vectors [7–9], primate ES cells are not efficiently transduced by these methods [10]. Lentiviral vectors can transduce both dividing and non-dividing cells and long-term expression of the transgene is stable in a wide range of target cells [11–13]. We have described the highly efficient transfer of a gene into cynomolgus monkey undifferentiated ES cells using a lentivirus vector based on simian immunodeficiency virus (SIV) [14].

The present study examines the differentiation of cynomolgus ES cells into functional cardiomyocytes and determines the efficiency and stability of gene transduction into these cardiomyocytes using an SIV-based lentiviral vector encoding the enhanced green fluorescence protein (EGFP) gene. We also evaluate the survival of transplanted cardiomyocytes derived from cynomolgus ES cells in the injured myocardium of a rat myocardial infarction model.

Materials and methods

Cell preparations

The cynomolgus monkey ES cell line CMK6 [6] was cultured in DMEM/F12 (Sigma, St. Louis, USA) on a mouse embryonic fibroblast feeder layer that was mitotically inactivated with mitomycin C (Kyowa, Tokyo, Japan). The medium was supplemented with 0.1 mM 2-mercaptoethanol (Sigma), 2 mM glutamine (Invitrogen, Carlsbad, USA), 1 mM sodium pyruvate (Invitrogen) and 15% fetal bovine serum (FBS, ICN Biomedicals, Inc., Ohio, USA). To induce differentiation, ES cells were dispersed into small clumps using collagenase IV (Wako, Osaka, Japan), transferred to plastic Petri dishes and suspension-cultured for 10 days. During this period, the cells aggregated to form embryoid bodies (EBs), which were then plated on plastic plates, and the appearance of spontaneous contractions was observed under a microscope. Rat neonatal cardiomyocytes were prepared from cardiac ventricles of 1-day-old Sprague-Dawley rats as described previously [15]. The cells were grown in DMEM (Sigma) supplemented with 10% FBS (ICN Biomedicals, Inc.), and 1% penicillin/streptomycin solution (Invitrogen). All experiments were carried out in full compliance with the institutional animal care and use committee of the Jichi Medical School.

RT-PCR

Total RNA from undifferentiated ES cells, contracting EBs, and heart tissue of an adult cynomolgus monkey that was killed for unrelated reasons was extracted using a RNA extraction kit (Qiagen, Hilden, Germany) according to the manufacturer's instructions. Complementary DNA synthesized from 1 μg total RNA using SuperScript II reverse transcriptase (Life Technologies, Gaithersburg, MD, USA) was amplified by PCR using the following primers selective for human cardiac genes (oligonucleotide sequences are given in brackets in the order of anti-sense, sense primer followed by the annealing temperature, cycles used for PCR and length of the amplified fragment): cardiac troponin T (cTnT, 5′-GGCAGCGGAAGAGGATGCTGAA and 5′-GAGGCACCAAGTTGGGCATGAACGA; 60 °C; 35 cycles; 150 bp), atrial myosin light chain (MLC-2A, 5′-ACAGAGTTTATTGAGGTGCCCC and 5′-AAGGTGAAGTG-TCCCAGAGG; 61 °C; 35 cycles; 381 bp), ventricular myosin light chain (MLC-2V, 5′-TATTGGAACATGGCCTC-TGGAT and 5′-GGTGCTGAAGGCTGATTACGTT; 61 °C; 35 cycles; 382 bp), α-myosin heavy chain (αMHC, 5′-GTCATTGCTGAAACCGAGAATG and 5′-GCAAAGTACTG-GATGACACGCT; 61 °C; 40 cycles; 413 bp), octamer-binding protein 4 (Oct-4, 5′-GAGAACAATGAGAACCTTC-AGGAGA and 5′-TTCTGGCGCCGGTTACAGAACCA; 55 °C; 35 cycles; 219 bp), and glyceraldehyde-3-phosphate dehydrogenase (GAPDH, 5′-ATGCCAGTGAGCTTCCCGTT and 5′-CATCACCATCTTCCAGGAGC; 58 °C; 30 cycles; 473 bp).

Electron microscopy

For transmission electron microscopy, tissues were fixed in 2% paraformaldehyde/2.5% glutaraldehyde in 0.1 M phosphate-buffered saline (PBS), pH 7.4, at 4 °C for 24 h, postfixed in 1% OsO_4 in PBS for 1 h, dehydrated in a graded ethanol series and embedded in Epon 812. Thin (60–90 nm) sections were stained with uranyl acetate and lead citrate, and observed using a JEM-2000EX transmission electron microscope operating at 80 kV.

Intracellular calcium transience

Intracellular calcium transience of the EBs and rat neonatal cardiomyocytes was measured as described previously [16]. Briefly, cells were loaded with fura-2-AM (Dojin Biochemicals, Kumamoto, Japan), washed and transferred to the chamber of a fluorescence spectrophotometer (CAF-100; Japan Spectroscopic Co., Tokyo, Japan). Fura-2 fluorescence was measured using a dual wavelength system. Fluorescence was monitored at 500 nm, with excitation at 340 and 380 nm in the ratio mode. After achieving a stable fluorescence signal, the cells were stimulated with 100 nM angiotensin II (Sigma) or endothelin-1 (Peptide Institute Inc., Osaka, Japan). The cells pretreated with [Sar^1,Ile^8]-angiotensin II (non-selective antagonist; Peptide Institute Inc.) or CV-11 974

(angiotensin II type 1 receptor antagonist; kind gift from Takeda Chemical Industries, Ltd., Osaka, Japan) were also stimulated with angiotensin II.

Immunohistochemical staining

Contracting areas in EBs were mechanically dissected using a sterile micropipette. The samples were fixed in 4% paraformaldehyde in 0.1 M PBS (pH 7.4) containing 8% sucrose at 4 °C for 4 h, washed with PBS containing 10, 20, and 30% sucrose in that order, embedded in OCT compound (Miles Laboratory, IN, USA), frozen in liquid nitrogen and cut into thin (8–10 μm) sections. We incubated the sections with monoclonal antibodies against human cardiac troponin I (cTnI) and cardiac myosin (both from Biogenesis, England, UK; diluted 1 : 200) for 1 h at room temperature. These anti-human antibodies cross-react against cynomolgus monkey cardiomyocytes but not against rat cardiomyocytes. Texas red labelled anti mouse IgG (Vector, Burlingame, CA, USA) was the secondary antibody. Samples were fixed in 4% paraformaldehyde in PBS for 20 min and immersed in 4′,6-diamidino-2-phenylindole (DAPI, 500 ng/ml; Sigma) containing Tris buffer (pH 7.4) for 10 min at room temperature to stain nuclei.

Vector construction and transduction

The SIV vector expressing the EGFP gene (Clontech, CA, USA) was produced by transient transfection into 293T cells as described [17]. Briefly, the envelope plasmid (pVSV-G; Clontech) encoding the vesicular stomatitis virus G (VSV-G) protein, the packaging plasmid (pCAGGS/Sagm-gtr), and the vector plasmid (pBS/CG2-Rc/s-CMV-ΔU) expressing the EGFP gene under the control of the cytomegalovirus (CMV) promoter were transfected into 293T cells and supernatants were harvested 48 h later. The SIV vector was concentrated by centrifugation of the supernatants at 42 500 *g* for 90 min and the titer assessed by fluorescence activated cell sorting (FACS) using 293T cells as targets was 1.87×10^8 TU/ml.

Spontaneously contracting EBs were transduced with SIV vector expressing the EGFP gene at a multiplicity of infection (MOI) of 100. Cells were washed with PBS 10 h later and incubated in fresh medium for 7–14 days. Contracting EBs were micro-dissected with a sterile micropipette and prepared for immunohistological analysis. Other dissected cells were enzymatically dispersed in trypsin/EDTA solution (0.05% trypsin, 0.53 mM EDTA; Invitrogen) for 7 min at 37 °C and resuspended in DMEM/F12 for use in cell transplantation experiments. To determine the transduction efficiency with the SIV vector, some dissociated cells were centrifuged with Cytospin and stained with anti-cTnI antibody. We then calculated the ratio (%) of EGFP-positive cells among cTnI-immunoreactive cells.

Cell transplantation in a rat myocardial infarction model

Immunodeficient (F344/N *rnu/rnu*) nude rats (male, initial body weight 140–180 g) were used ($n = 4$) to avoid graft-versus-host disease. Left thoracotomy proceeded under general anesthesia, then the pericardium was opened and the left descending coronary artery was ligated. Cynomolgus ES-cell-derived cardiomyocytes expressing EGFP (1×10^5 cells/50 μl) were implanted in the injured myocardium 30 min after myocardial infarction induction. Two weeks later, rats were killed and hearts were extracted for immunohistological study. All experiments in this study were performed in accordance with the Jichi Medical School Guide for Laboratory Animals.

Statistical analysis

Results are presented as mean ± SD. For comparisons between multiple groups, we determined the significance of differences between group means by ANOVA using the least significant difference for multiple comparisons. Differences at values of $p < 0.05$ were considered to be statistically significant.

Results

Differentiation of cynomolgus ES cells into cardiomyocytes

Rhythmically contracting areas appeared between 3 and 10 days after plating EBs on plastic plates, and were maintained for 3–4 weeks. Figure 1A shows that the ratio of EBs containing beating areas as a function of time after plating was 8.7% (of 751 EBs) at 14 days.

We investigated the expression of cardiac-specific genes in spontaneously contracting EBs. The RT-PCR results revealed that these cells expressed cTnT, MLC-2A, MLC-2V, and αMHC (Figure 1B). In contrast, Oct-4, a marker of undifferentiated ES cells, was expressed in undifferentiated ES cells, but not in contracting EBs or cynomolgus heart tissues. Light microscopy showed that the contracting areas were composed mainly of round or rod-shaped mononuclear cells. Myofibers were detected in the high power light microscopy image stained with toluidine blue (Figure 2A). Transmission electron microscopy revealed that these cells had the mature sarcomeric organization and desmosome structure of cardiomyocytes (Figures 2B–2D). To further elucidate whether these cells have functional features as cardiomyocytes, we measured the effect of angiotensin II or endothelin-1 on intracellular calcium transience. Intracellular calcium transience was obviously stimulated with angiotensin II or endothelin-1. The angiotensin II stimulated effect was completely inhibited by pretreatment with [Sar^1,Ile^8]-angiotensin II